Group-Blind Multiuser Detection for Uplink CDMA

Xiaodong Wang, *Member, IEEE*, and Anders Høst-Madsen, *Member, IEEE*

***Abstract*— The recently developed blind techniques for multiuser detection in code division multiple access (CDMA) systems lead to several near–far resistant adaptive receivers for demodulating a given user's data with the prior knowledge of only the spreading sequence of that user. In the CDMA uplink, however, typically the base station receiver has the knowledge of the spreading sequences of all the users within the cell, but not that of the users from other cells. In this paper, group-blind techniques are developed for multiuser detection in such scenarios. These new techniques make use of the spreading sequences and the estimated multipath channels of all known users to suppress the intracell interference, while blindly suppressing the intercell interference. Several forms of group-blind linear detectors are developed based on different criteria. Moreover, group-blind multiuser detection in the presence of correlated noise is also considered. In this case, two receiving antennas are needed for channel estimation and signal separation. Simulation results demonstrate that the proposed group-blind linear multiuser detection techniques offer substantial performance gains over the blind linear multiuser detection methods in a CDMA uplink environment.**

***Index Terms*— Correlated noise, code division multiple access (CDMA) uplink, group-blind multiuser detection, multipath.**

I. Introduction

CONSIDERABLE recent research in the field of multiuser detection [21] has been focused on adaptive multiuser detection [7]. In particular, a blind adaptive multiuser detection method has been proposed in [6], which allows one to use a multiuser detector [i.e., the linear minimum mean-square error (MMSE) detector] for a given user with no prior knowledge beyond that required for implementation of the conventional detector for that user. This method has been extended to address a number of other channel impairments, such as narrowband interference [15], [16], channel dispersion [19], [20], fading channels [2], [11], [22], [29], and synchronization [13], [14]. More recently, a subspace approach to blind adaptive multiuser detection has been proposed in [25]. This new technique exhibits some advantages over the method in [6]. Moreover, within the subspace framework, extensions have been made to fading channels [17], [23], dispersive channels [24], and antenna array spatial processing [25] for blind adaptive joint channel/array response estimation, multiuser detection, and equalization. Another salient feature of the subspace approach is that it can be combined with M-regression techniques to achieve blind adaptive robust multiuser detection in non-Gaussian ambient noise channels [27].

These blind multiuser detection techniques are especially useful for interference suppression in code division multiple access (CDMA) downlinks, where a mobile receiver knows only its own spreading sequence. In CDMA uplinks, however, typically the base station receiver has the knowledge of the spreading sequences of a group of users, e.g., the users within its cell, but not that of the users from other cells. It is natural to expect that some performance gains can be achieved over the blind methods (which exploits only the spreading sequence of the given user) in detecting each individual user's data if the information about the spreading sequences of the other known users is also exploited. Such an idea was first explored in [8]–[10], where a number of linear and nonlinear detectors were developed for synchronous CDMA systems, which improved the subspace blind method in [25] by taking into account the knowledge of the spreading sequences of other users within the same cell. In this paper, we generalize the idea in [9] and [10] and develop linear group-blind multiuser detection techniques that suppress the intracell interference, using the knowledge of the spreading sequences and the estimated multipath channels of a group of known users, while suppressing the intercell interference blindly. Several forms of such group-blind detectors are developed based on different criteria. It is shown through simulations that the proposed group-blind techniques significantly outperform the blind methods in a CDMA uplink environment.

Another issue addressed in this paper is blind and group-blind multiuser detection in the presence of correlated ambient channel noise. Although it is usually assumed that the ambient noise is temporally white, in practice, such an assumption may be violated, due to the interference from some narrowband sources, for instance. We extend the ideas of blind and group-blind multiuser detection to the case where the noise is correlated. In this case, it is assumed that the signal is received by two antennas well separated so that the output noise is spatially uncorrelated. Blind and group-blind multiuser detectors based on the canonical correlation decomposition (CCD) method is developed. Simulation results show again that the group-blind detector offers substantial performance gains over the blind detector in correlated ambient noise.

The rest of the paper is organized as follows. In Section II, the multipath CDMA signal model is presented. In Section III, blind channel estimation methods in the presence of both white and correlated noise are discussed. In Section IV, subspace blind linear detectors in both white and correlated noise are presented. In Section V, several forms of group-blind detectors are defined based on different criteria, and their

Manuscript received February 16, 1999; revised July 23, 1999.

X. Wang is with the Department of Electrical Engineering, Texas A&M University, College Station, TX 77843 USA.

A. Høst-Madsen is with TRLabs and the Department of Electrical Engineering, University of Calgary, Calgary, Alberta T2L 2K7 Canada.

Publisher Item Identifier S 0733-8716(99)08956-8.

expressions are derived for both white and correlated noise. In Section VI, simulation examples are provided to demonstrate the performance of the various algorithms developed in this paper. Section VII contains the conclusions.

II. Signal Model

Consider a K-user binary communication system, employing normalized modulation waveforms $s_1, s_2, \ldots, s_K$ and signaling through their respective multipath channels with additive Gaussian noise. The transmitted signal due to the kth user is given by

$$x_k(t) = A_k \sum_{i=0}^{M-1} b_k[i] s_k(t - iT - d_k) \tag{1}$$

where M denotes the length of the data frame; T denotes the information symbol interval and A_k, $\{b_k(i)\}$, and d_k $(0 \le d_k < T)$ denote the amplitude, symbol stream, and delay of the kth user's signal, respectively. It is assumed that for each $k, \{b_k(i)\}$ is a collection of independent equiprobable ± 1 random variables, and the symbol streams of different users are independent. For the direct sequence-spread spectrum (DS-SS) multiple access format, the user signaling waveforms are of the form

$$s_k(t) = \sum_{j=0}^{N-1} c_k[j]\, \psi(t - jT_c), \qquad 0 \le t \le T \tag{2}$$

where N is the processing gain, $\{c_k[j]\}_{j=0}^{N-1}$ is a signature sequence of ± 1 s assigned to the kth user, and ψ is a chip waveform of duration $T_c = (T/N)$. The kth user's signal $x_k(t)$ propagates through a multipath channel whose impulse response is given by

$$g_k(t) = \sum_{l=1}^{L} \alpha_{kl} \delta(t - \tau_{kl}) \tag{3}$$

where L is the total number of paths in the channel, and α_{kl} and τ_{kl} are the complex path gain and the delay of the kth user's lth path, respectively. Throughout this paper, it is assumed that the channel is slowly time varying, such that the path gains and delays remain constant over the duration of one signal frame (MT). Using (1) and (3), the received signal component due to the kth user is then given by

$$\begin{aligned} y_k(t) &= x_k(t) * g_k(t) \\ &= \sum_{i=0}^{M-1} b_k[i] \underbrace{[A_k s_k(t - iT - d_k) * g_k(t)]}_{h_k(t-iT)} \end{aligned} \tag{4}$$

where $*$ denotes convolution, and where using (2)

$$\begin{aligned} h_k(t) &\triangleq A_k s_k(t - d_k) * g_k(t) \\ &= \sum_{j=0}^{N-1} c_k[j] \underbrace{\left[A_k \sum_{l=1}^{L} \alpha_{kl} \psi(t - jT_c - d_k - \tau_{kl}) \right]}_{\overline{g}_k(t - jT_c)}. \end{aligned} \tag{5}$$

In (5), $\overline{g}_k(t)$ is the composite channel response, taking into account the effects of transmitter power, chip pulse waveform, and the multipath channel, given by

$$\overline{g}_k(t) \triangleq A_k \sum_{l=1}^{L} \alpha_{kl} \psi(t - d_k - \tau_{kl}). \tag{6}$$

Since $\psi(t)$ is zero outside the interval $[0, T_c]$, $\overline{g}_k(t)$ is zero outside the interval $[d_k + \tau_{k1}, d_k + \tau_{kL} + T_c]$. Hence, the composite signature waveform $h_k(t)$ of the kth user, defined in (5), is zero outside the interval $[d_k + \tau_{k1}, d_k + \tau_{kL} + T]$.

The total received signal at the base station receiver is the superposition of the signals of the K users, plus additive Gaussian noise, given by

$$r(t) = \sum_{k=1}^{K} y_k(t) + v(t) \tag{7}$$

where $v(t)$ is a zero mean complex Gaussian noise process. At the receiver, the received signal $r(t)$ is sampled at a multiple (p) of the chip-rate, i.e., the sampling time interval is $\Delta = (T_c/p) = (T/P)$, where $P \triangleq pN$ is the total number of samples per symbol interval. The nth received signal sample during the ith symbol is given by

$$\begin{aligned} r[i,n] &\triangleq r((iP + n)\Delta) = r(iT + n\Delta) \\ &= \sum_{k=1}^{K} \underbrace{y_k(iT + n\Delta)}_{y_k[i,n]} + \underbrace{v(iT + n\Delta)}_{v[i,n]}. \end{aligned} \tag{8}$$

Denote $\iota_k \triangleq \lceil d_k + \tau_{kL} + T_c/T \rceil$. Then using (4), we have

$$\begin{aligned} y_k[i,n] &\triangleq y_k(iT + n\Delta) = \sum_{j=0}^{M-1} b_k[j]\, h_k(iT + n\Delta - jT) \\ &= \sum_{j=i-\iota_k}^{i} b_k[j] \underbrace{h_k(iT + n\Delta - jT)}_{h_k[i-j,n]} \\ &= \sum_{j=0}^{\iota_k} h_k[j,n]\, b_k[i-j] \end{aligned} \tag{9}$$

where (9) follows from the fact that $h_k(t)$ is zero outside the interval $[0, (\iota_k + 1)T]$. Hence, for the kth user, (8) can be written as

$$\begin{aligned} r[i,n] = h_k[0,n] b_k[i] &+ \underbrace{\sum_{j=1}^{\iota_k} h_k[j,n] b_k[i-j]}_{\text{ISI}} \\ &+ \underbrace{\sum_{k' \ne k} y_{k'}[i,n]}_{\text{MAI}} + v[i,n]. \end{aligned} \tag{10}$$

In (10), the first term contains the ith bit of the kth user; the second term contains the intersymbol interference (ISI) from the previous bits of the kth user; the third term contains the multiple access interference (MAI) from other users, and the last term is the ambient channel noise. Denote

$$\underbrace{\underline{r}[i]}_{P\times 1} \triangleq \begin{bmatrix} r[i,0] \\ \vdots \\ r[i,P-1] \end{bmatrix}$$

$$\underbrace{\underline{v}[i]}_{P\times 1} \triangleq \begin{bmatrix} v[i,0] \\ \vdots \\ v[i,P-1] \end{bmatrix}$$

$$\underbrace{\underline{b}[i]}_{K\times 1} \triangleq \begin{bmatrix} b_1[i] \\ \vdots \\ b_K[i] \end{bmatrix}$$

$$\underbrace{\underline{H}[j]}_{P\times K} \triangleq \begin{bmatrix} h_1[j,0] & \cdots & h_K[j,0] \\ \vdots & \vdots & \vdots \\ h_1[j,P-1] & \cdots & h_K[j,P-1] \end{bmatrix}$$
$$j = 0,1,\ldots,\iota_k.$$

Then from (8) and (9), we have

$$\underline{r}[i] = \underline{H}[i] * \underline{b}[i] + \underline{v}[i]. \tag{11}$$

Define $\iota \triangleq \max_{1\le k\le K}\ \{\iota_k\}$. By stacking m successive received sample vectors, we further define the following quantities

$$\underbrace{\boldsymbol{r}[i]}_{Pm\times 1} \triangleq \begin{bmatrix} \underline{r}[i] \\ \vdots \\ \underline{r}[i+m-1] \end{bmatrix}$$

$$\underbrace{\boldsymbol{v}[i]}_{Pm\times 1} \triangleq \begin{bmatrix} \underline{v}[i] \\ \vdots \\ \underline{v}[i+m-1] \end{bmatrix}$$

$$\underbrace{\boldsymbol{b}[i]}_{r\times 1} \triangleq \begin{bmatrix} \underline{b}[i-\iota] \\ \vdots \\ \underline{b}[i+m-1] \end{bmatrix}$$

$$\underbrace{\boldsymbol{H}}_{Pm\times r} \triangleq \begin{bmatrix} \underline{H}[\iota] & \cdots & \underline{H}[0] & \cdots & \mathbf{0} \\ \vdots & \ddots & \ddots & \ddots & \vdots \\ \mathbf{0} & \cdots & \underline{H}[\iota] & \cdots & \underline{H}[0] \end{bmatrix}$$

where $r \triangleq K(m+\iota)$. We can then write (11) in a matrix forms as

$$\boldsymbol{r}[i] = \boldsymbol{H}\,\boldsymbol{b}[i] + \boldsymbol{v}[i]. \tag{12}$$

As will be discussed in Section III-B, the smoothing factor m is chosen according to $m = \lceil (P+K)/(P-K) \rceil \iota$. Note that for such m, the matrix $\boldsymbol{H}$ is a "tall" matrix, i.e., $Pm \ge r \triangleq K(m+\iota)$.

III. Blind Channel Estimation

In this section, we consider the problem of estimating the physical channel of a given user from the received signal, based on the knowledge of the spreading sequence of that user. The estimated user channels are used to form linear blind and group-blind multiuser detectors, as will be discussed in Sections IV and V. The discrete-time channel model is presented in Section III-A. Blind channel estimation techniques in the presence of white and correlated ambient noise are discussed in Sections III-B and III-C, respectively.

A. Discrete-Time Channel Model

From (5) and (9), we have

$$\begin{aligned} h_k[j,n] &\triangleq h_k(jT + n\Delta) \\ &= \sum_{l=0}^{N-1} c_k[l]\overline{g}_k(jT + n\Delta - lT_c), \\ &\qquad j = 0,\ldots,\iota_k; \quad n = 0,\ldots,P-1. \end{aligned} \tag{13}$$

Decimate $h_k[j,n]$ into p sub-sequences as

$$\begin{aligned} h_{k,q}[j,i] &\triangleq h_k[j,q+pi] = h_k(jT + (q+pi)\Delta) \\ &= \sum_{l=0}^{N-1} c_k[l]\overline{g}_k(jT + (q+pi)\Delta - lT_c) \\ &= \sum_{l=0}^{N-1} c_k[l] \underbrace{\overline{g}_k(q\Delta + (jN+i-l)p\Delta)}_{\overline{g}_k[(jN+i-l)p+q] \triangleq \overline{g}_{k,q}(jN+i-l)} \\ &= \sum_{l=0}^{N-1} c_k[l]\overline{g}_{k,q}(jN+i-l), \\ &\qquad j = 0,\ldots,\iota_k; \quad i = 0,\ldots,N-1; \\ &\qquad q = 0,\ldots,p-1 \end{aligned} \tag{14}$$

where the fourth equality follows from the fact that $T = NT_c$ and $T_c = p\Delta$. The sequence $\{\overline{g}_k[i]\}$ is obtained by sampling the composite channel response $\overline{g}_k(t)$ given in (6), at rate $(1/\Delta) = (p/T_c)$

$$\begin{aligned} \overline{g}_k[i] &\triangleq \overline{g}_k(i\Delta) = A_k \sum_{l=1}^{L} \alpha_{kl}\psi(i\Delta - d_k - \tau_{kl}), \\ &\qquad i = 0,\ldots,p\mu_k - 1. \end{aligned} \tag{15}$$

The length $(p\mu_k)$ of the sequence $\{\overline{g}_k[i]\}$ is determined by the length of support of $\overline{g}_k(t)$. Since $\overline{g}_k(t)$ is nonzero only on the interval $[d_k + \tau_{k1}, d_k + \tau_{kL} + T_c]$, we have

$$\begin{aligned} \mu_k &= \left\lceil \frac{d_k + \tau_{kL} + T_c}{p\Delta} \right\rceil \\ &= \left\lceil \frac{d_k + \tau_{kL} + T_c}{T} \cdot \frac{T}{T_c} \right\rceil \le \iota_k N. \end{aligned} \tag{16}$$

The sequences $\{\overline{g}_{k,q}[i]\}$ in (14) is obtained by down sampling the sequence $\{\overline{g}_k[i]\}$ by a factor of p, i.e.,

$$\begin{aligned} \overline{g}_{k,q}[i] = \overline{g}_k[ip+q], &\qquad i = 0,\ldots,\mu_k - 1; \\ &\qquad q = 0,\ldots,p-1. \end{aligned} \tag{17}$$

From (14), we have

$$\begin{aligned} &\{h_{k,q}[0,0],\cdots,h_{k,q}[0,N-1],\ldots\ldots,h_{k,q}[\iota_k,0], \\ &\quad \ldots,h_{k,q}[\iota_k,N-1]\} \\ &\quad = \{c_k[0],\ldots,c_k[N-1]\} * \{\overline{g}_{k,q}[0],\ldots,\overline{g}_{k,q}[\mu_k - 1]\}. \end{aligned} \tag{18}$$

Denote

$$\underbrace{\boldsymbol{h}_{k,q}}_{(\iota_k+1)N\times 1} \triangleq \begin{bmatrix} h_{k,q}[0,0] \\ \vdots \\ h_{k,q}[0,N-1] \\ \vdots \\ h_{k,q}[\iota_k,0] \\ \vdots \\ h_{k,q}[\iota_k,N-1] \end{bmatrix}$$

$$\underbrace{\overline{\boldsymbol{g}}_{k,q}}_{\mu_k\times 1} \triangleq \begin{bmatrix} \overline{g}_{k,q}[0] \\ \vdots \\ \overline{g}_{k,q}[\mu_k-1] \end{bmatrix}$$

$$\underbrace{\boldsymbol{C}_k}_{(\iota_k+1)N\times\mu_k} \triangleq \begin{bmatrix} c_k[0] & & \\ c_k[1] & \ddots & \\ \vdots & \ddots & c_k[0] \\ \vdots & & c_k[1] \\ c_k[N-1] & & \vdots \\ & \ddots & \vdots \\ & & c_k[N-1] \end{bmatrix}.$$

Then (18) can be written in a matrix form as

$$\boldsymbol{h}_{k,q} = \boldsymbol{C}_k\,\overline{\boldsymbol{g}}_{k,q}. \tag{19}$$

Finally, denote

$$\underbrace{\boldsymbol{h}_k}_{(\iota_k+1)P\times 1} \triangleq [h_k[0,0]\cdots h_k[0,P-1]\cdots h_k[\iota_k,0] \cdots h_k[\iota_k,P-1]]^T$$

$$\underbrace{\overline{\overline{g}}_k}_{p\mu_k\times 1} \triangleq [\overline{g}_k[0]\cdots\overline{g}_k[p\mu_k-1]]^T.$$

Then we have

$$\boldsymbol{h}_k = \tilde{\boldsymbol{C}}_k\,\overline{\boldsymbol{g}}_k \tag{20}$$

where $\tilde{\boldsymbol{C}}_k$ is an $[(\iota_k+1)P \times p\mu_k]$ matrix formed from the spreading code of kth user. For instance, when the oversampling factor $p=2$, we have $\tilde{\boldsymbol{C}}_k$, as shown at the bottom of the page. For other values of p, the matrix $\tilde{\boldsymbol{C}}_k$ is similarly constructed. Suppose that user k is the user of interest and its spreading sequence $\{c_k[0],\ldots,c_k[N-1]\}$ is known to the receiver (and therefore $\tilde{\boldsymbol{C}}_k$ is known). We next consider the problem of estimating the channel vector $\overline{\boldsymbol{g}}_k$ in (20) based on the received signal $\boldsymbol{r}[i]$ in (12).

B. Channel Estimation in White Noise

When the ambient noise is white, i.e., $E\{\boldsymbol{v}[i]\boldsymbol{v}[i]^H\} = \sigma^2\boldsymbol{I}_{Pm}$ [here $\boldsymbol{I}_{Pm}$ denotes a $(Pm\times Pm)$ identity matrix], the autocorrelation matrix of the received signal $\boldsymbol{r}[i]$ in (12) is

$$\boldsymbol{R} \triangleq E\{\boldsymbol{r}[i]\boldsymbol{r}[i]^H\} = \boldsymbol{H}\boldsymbol{H}^H + \sigma^2\boldsymbol{I}_{Pm} \tag{21}$$

$$= \boldsymbol{U}_s\boldsymbol{\Lambda}_s\boldsymbol{U}_s^H + \sigma^2\boldsymbol{U}_n\boldsymbol{U}_n^H \tag{22}$$

where (22) is the eigendecomposition of $\boldsymbol{R}$. Since the matrix $\boldsymbol{H}$ has full column rank $r \triangleq K(m+\iota)$, the matrix $(\boldsymbol{H}\boldsymbol{H}^H)$ in (21) has rank r. Therefore, in (22) $\boldsymbol{\Lambda}_s = \text{diag}(\lambda_1,\ldots,\lambda_r)$ contains the r largest eigenvalues of $\boldsymbol{R}$ in descending order (i.e., $\lambda_1 \ge \lambda_2 \ge \cdots \ge \lambda_r > \sigma^2$); $\boldsymbol{U}_s = [\boldsymbol{u}_1 \;\cdots\; \boldsymbol{u}_r]$ contains the corresponding orthonormal eigenvectors; and $\boldsymbol{U}_n = [\boldsymbol{u}_{r+1}\cdots\boldsymbol{u}_{Pm}]$ contains the $(Pm-r)$ orthonormal eigenvectors that correspond to the eigenvalue σ^2. It is easy to see that range$(\boldsymbol{H})$ = range$(\boldsymbol{U}_s)$. The column space of $\boldsymbol{U}_s$ is called the signal subspace and its orthogonal complement, the noise subspace, is spanned by the columns of $\boldsymbol{U}_n$.

Denote $\mathbf{1}_l$ as a $[K(m+\iota)]$-vector with all-zero entries except for the lth entry, which is one. Define $\overline{\boldsymbol{h}}_k \triangleq \boldsymbol{H}\mathbf{1}_{K\iota+k}$. Then by (20) we have

$$\overline{\boldsymbol{h}}_k = \begin{bmatrix} \boldsymbol{h}_k \\ \mathbf{0}_{(m-\iota-1)P\times 1} \end{bmatrix} = \underbrace{\begin{bmatrix} \tilde{\boldsymbol{C}}_k \\ \mathbf{0}_{(m-\iota_k-1)P\times p\mu_k} \end{bmatrix}}_{\overline{\boldsymbol{C}}_k} \overline{\boldsymbol{g}}_k. \tag{23}$$

The channel response $\overline{\boldsymbol{g}}_k$ can be estimated by exploiting the orthogonality between the signal subspace and the noise subspace [3], [12], [18], [24]. Specifically, since $\boldsymbol{U}_n$ is orthogonal to the column space of $\boldsymbol{H}$, and $\overline{\boldsymbol{h}}_k$ is in the column space of $\boldsymbol{H}$, we have

$$\boldsymbol{U}_n^H\overline{\boldsymbol{h}}_k = \boldsymbol{U}_n^H\overline{\boldsymbol{C}}_k\overline{\boldsymbol{g}}_k = \mathbf{0}. \tag{24}$$

$$\underbrace{\tilde{\boldsymbol{C}}_k}_{2(\iota_k+1)N\times 2\mu_k} = \begin{bmatrix} c_k[0] & & & & & \\ 0 & c_k[0] & & & & \\ c_k[1] & 0 & c_k[0] & & & \\ 0 & c_k[1] & 0 & c_k[0] & & \\ \vdots & \ddots & \ddots & \ddots & \ddots & \\ \vdots & & \ddots & \ddots & \ddots & c_k[0] \\ c_k[N-1] & & & 0 & c_k[1] & 0 \\ & c_k[N-1] & & & 0 & c_k[1] \\ & & \ddots & & & 0 \\ & & & \ddots & & \vdots \\ & & & & \ddots & \vdots \\ & & & & & c_k[N-1] \end{bmatrix}.$$

Hence, an estimate of the channel response $\bar{\boldsymbol{g}}_k$ can be obtained by computing the minimum eigenvector of the matrix $(\overline{\boldsymbol{C}}_k^T \boldsymbol{U}_n \boldsymbol{U}_n^H \overline{\boldsymbol{C}}_k)$. A necessary condition for such a channel estimate to be unique is that the matrix $\boldsymbol{U}_n^H \overline{\boldsymbol{C}}_k$ has rank $(p\mu_k - 1)$, which necessitates this matrix be tall, i.e., $[Pm - K(m+\iota)] \geq p\mu_k$. Since $\mu_k \leq \iota_k N$ [cf. (16)], we therefore choose m to satisfy

$$Pm - K(m+\iota) \geq \iota P \geq \iota_k N p \geq p\mu_k. \tag{25}$$

That is, the smoothing factor is chosen to be $m = \lceil (P+K)/(P-K) \rceil \iota$.

Remark 1: Note that the estimated channel vector $\bar{\boldsymbol{g}}_k$ contains the information about both the timings and the complex gains of the multipath channel of the kth user. Hence, this channel estimation method does not need the timing information $\{\tau_{kl}\}_{l=1}^L$ of the multipath channel of the given user. The only prior knowledge it requires is the spreading waveform and the delay spread (in terms of number of symbol intervals) of that user. (For practical CDMA systems, the delay spread is usually one symbol interval.)

C. Channel Estimation in Correlated Noise

We next consider channel estimation in the presence of correlated ambient noise. The key assumption here is that the signal is received by two antennas well separated so that the noise is spatially uncorrelated. Then the two augmented received signal vectors at the two antennas can be written respectively as

$$\boldsymbol{r}^1[i] = \boldsymbol{H}^1 \boldsymbol{b}[i] + \boldsymbol{v}^1[i] \quad \text{and} \tag{26}$$

$$\boldsymbol{r}^2[i] = \boldsymbol{H}^2 \boldsymbol{b}[i] + \boldsymbol{v}^2[i] \tag{27}$$

where $\boldsymbol{H}^1$ and $\boldsymbol{H}^2$ contain the channel information corresponding to the respective antennas. It is assumed that the two antennas are well separated so that the ambient noise is spatially uncorrelated, i.e., $E\{\boldsymbol{v}^1[i]\boldsymbol{v}^2[i]^H\} = \boldsymbol{0}$. Denote $\boldsymbol{\Sigma}^j = E\{\boldsymbol{v}^j[i]\boldsymbol{v}^j[i]^H\}, j = 1, 2$. Denote further

$$\boldsymbol{R}_{jj} \triangleq E\{\boldsymbol{r}^j[i]\boldsymbol{r}^j[i]^H\} = \boldsymbol{H}^j \boldsymbol{H}^{jH} + \boldsymbol{\Sigma}^j \quad j = 1, 2 \tag{28}$$

$$\boldsymbol{R}_{21}^H \triangleq E\{\boldsymbol{r}^1[i]\boldsymbol{r}^2[i]^H\} = \boldsymbol{H}^1 \boldsymbol{H}^{2H}. \tag{29}$$

As before, in order to estimate the kth user's channels $\bar{\boldsymbol{h}}_k^j = \overline{\boldsymbol{C}}_k \bar{\boldsymbol{g}}_k^j, j = 1, 2$, we need to first estimate the noise subspace null$(\boldsymbol{H}^j)^T$ which is orthogonal to the signal subspace range$(\boldsymbol{H}^j)$. Following [28], such a noise subspace estimate can be obtained by using the canonical correlation decomposition (CCD) of the matrix $\boldsymbol{R}_{12}$.

Assume that the matrices $\boldsymbol{R}_{11}$ and $\boldsymbol{R}_{22}$ are both positive definite. The CCD of the matrix $\boldsymbol{R}_{12}$ is given by [1]

$$\boldsymbol{R}_{11}^{-1/2} \boldsymbol{R}_{12} \boldsymbol{R}_{22}^{-1/2} = \boldsymbol{U}^1 \boldsymbol{\Gamma} \boldsymbol{U}^{2H} \quad \text{or} \tag{30}$$

$$\boldsymbol{R}_{11}^{-1} \boldsymbol{R}_{12} \boldsymbol{R}_{22}^{-1} = \underbrace{\boldsymbol{R}_{11}^{-1/2} \boldsymbol{U}^1}_{\boldsymbol{L}^1} \boldsymbol{\Gamma} \underbrace{\boldsymbol{U}^{2H} \boldsymbol{R}_{22}^{-1/2}}_{\boldsymbol{L}^{2H}}. \tag{31}$$

The $(Pm \times Pm)$ matrix $\boldsymbol{\Gamma}$ has the form $\boldsymbol{\Gamma} = \text{diag}(\gamma_1, \ldots, \gamma_r, 0, \ldots, 0)$, with $\gamma_1 \geq \cdots \geq \gamma_r > 0$. Partition the matrix $\boldsymbol{L}^j$ as

$$\boldsymbol{L}^j = [\boldsymbol{L}_s^j, \boldsymbol{L}_n^j] = [\boldsymbol{R}_{jj}^{-1/2} \boldsymbol{U}_s^j, \boldsymbol{R}_{jj}^{-1/2} \boldsymbol{U}_n^j] \tag{32}$$

where $\boldsymbol{L}_s^j$ and $\boldsymbol{L}_n^j$ are the first r columns and the last $(Pm-r)$ columns of $\boldsymbol{L}^j$, respectively. $\boldsymbol{U}^j$ is similarly partitioned into $\boldsymbol{U}_s^j$ and $\boldsymbol{U}_n^j$. We then have [28]

$$\text{null}(\boldsymbol{H}^j)^T = \text{range}(\boldsymbol{L}_n^j), j = 1, 2. \tag{33}$$

However, note that $\boldsymbol{L}_s^j$ does not necessarily span the signal subspace range$(\boldsymbol{H}^j)$ [28]. Finally, the kth user's channel $\bar{\boldsymbol{h}}_k^j$ can be estimated from the orthogonality relationship

$$\boldsymbol{L}_n^{jH} \bar{\boldsymbol{h}}_k^j = \boldsymbol{L}_n^{jH} \overline{\boldsymbol{C}}_k \bar{\boldsymbol{g}}_k^j = \boldsymbol{0}. \tag{34}$$

It has been shown that the CCD has the optimality of maximizing the correlation between the two sets of linearly transformed data [1]. Maximizing the correlation of the two data sets can yield the best estimate of the correlated (i.e., signal) part of the data. CCD makes use of the information of both $\boldsymbol{R}_{11}$ and $\boldsymbol{R}_{22}$ together with $\boldsymbol{R}_{12}$ and creates the maximum correlation between the two data sets. On the other hand, the noise subspace null$(\boldsymbol{H}^j)^T$ can also be estimated based on the singular value decomposition (SVD) of the matrix $\boldsymbol{R}_{12}$. However, since the SVD uses only the information $\boldsymbol{R}_{12}$ and does not create the maximum correlation between the two data sets, it yields inferior performance to that of the CCD. Indeed, in [26], two blind multiuser detectors in correlated noise, based on the SVD method and the CCD method, respectively, are compared in terms of bit error rate (BER). It is seen there that the CCD-based detector has much superior performance to the SVD-based detector.

IV. Blind Linear Multiuser Detectors

A linear detector for user k can be represented by a vector $\boldsymbol{w}_k \in \mathcal{C}^{Pm}$, which is applied to the received signal $\boldsymbol{r}[i]$ in (12), to compute the ith bit of the kth user, according to the following rule:

$$\hat{b}_k[i] = \text{sgn}\{\Re(\boldsymbol{w}_k^H \boldsymbol{r}[i])\}. \tag{35}$$

Due to the structure of the received signal $\boldsymbol{r}[i]$ given by (12), any reasonable linear detector should satisfy $\boldsymbol{w}_k \in \text{range}(\boldsymbol{H})$. This is because any component of $\boldsymbol{w}_k$ outside range$(\boldsymbol{H})$ will not affect the signal component in the detector output $(\boldsymbol{w}_k^H \boldsymbol{r}[i])$, but it will enhance the output noise level. Two forms of linear detectors are the linear zero-forcing detector and the linear minimum mean-square error (MMSE) detector, which are described next.

A. Subspace Blind Linear Detectors in White Noise

The linear zero-forcing detector for the kth user has the form of (35) with the weight vector $\boldsymbol{w}_k = \boldsymbol{d}_k$, such that both the MAI and the ISI are completely eliminated at the detector output, i.e., $\boldsymbol{d}_k^H \boldsymbol{H} = \boldsymbol{1}_{K\iota+k}^T$. It is given by

$$\boldsymbol{d}_k = \boldsymbol{H}^{\dagger H} \boldsymbol{1}_{K\iota+k} = \boldsymbol{H}(\boldsymbol{H}^H \boldsymbol{H})^{-1} \boldsymbol{1}_{K\iota+k} \tag{36}$$

where † denotes the pseudo-inverse. The linear MMSE detector for the kth user has the form of (35) with the weight vector

$\boldsymbol{w}_k = \boldsymbol{m}_k$, where $\boldsymbol{m}_k \in \mathcal{C}^{Pm}$ is chosen to minimize the output mean-square error (MSE), i.e.,

$$\boldsymbol{m}_k = \arg \min_{\boldsymbol{w} \in \mathcal{C}^{Pm}} E\{|b_k[i] - \boldsymbol{w}^H \boldsymbol{r}[i]|^2\} = \boldsymbol{R}^{-1}\overline{\boldsymbol{h}}_k \tag{37}$$

where $\boldsymbol{R} \triangleq E\{\boldsymbol{r}[i]\boldsymbol{r}[i]^H\} = \boldsymbol{H}\boldsymbol{H}^H + E\{\boldsymbol{v}[i]\boldsymbol{v}[i]^H\}$. As discussed in Section III-B, when the ambient noise is white, i.e., $E\{\boldsymbol{v}[i]\boldsymbol{v}[i]^H\} = \sigma^2 \boldsymbol{I}_{Pm}$, through an eigendecomposition of $\boldsymbol{R}$ [cf. (22)], the signal and noise subspaces can be identified. The two linear detectors (36) and (37) can be, respectively, expressed in terms of these signal subspace components, as [24], [25]

$$\boldsymbol{d}_k = \boldsymbol{U}_s(\boldsymbol{\Lambda}_s - \sigma^2 \boldsymbol{I}_r)^{-1}\boldsymbol{U}_s^H \overline{\boldsymbol{h}}_k, \tag{38}$$

$$\boldsymbol{m}_k = \boldsymbol{U}_s \boldsymbol{\Lambda}_s^{-1} \boldsymbol{U}_s^H \overline{\boldsymbol{h}}_k. \tag{39}$$

Since the signal subspace components ($\boldsymbol{U}_s$,$\boldsymbol{\Lambda}_s$, and σ^2), as well as the composite signature waveform of the given user $\overline{\boldsymbol{h}}_k$ can be estimated from the received signal, with the prior knowledge of only the spreading sequence of the given user, the detectors (38) and (39) are hence termed blind.

B. Subspace Blind Linear Detectors in Correlated Noise

As discussed in Section III-C, when the ambient noise is correlated, two antennas are needed at the receiver in order to estimate the channels. The linear MMSE detector for user k at antenna j is given by

$$\boldsymbol{m}_k^j = \boldsymbol{R}_{jj}^{-1}\overline{\boldsymbol{h}}_k^j = \boldsymbol{L}^j \boldsymbol{L}^{jH} \overline{\boldsymbol{h}}_k^j = \boldsymbol{L}_s^j \boldsymbol{L}_s^{jH} \overline{\boldsymbol{h}}_k^j \tag{40}$$

where $\boldsymbol{R}_{jj}$ and $\boldsymbol{L}^j$ are defined in (28) and (31), respectively. The second equality in (40) follows from the fact that $\boldsymbol{U}^j$ in (31) is a unitary matrix; the third equality follows from the partitioning $\boldsymbol{L}^j = [\boldsymbol{L}_s^j \boldsymbol{L}_n^j]$ in (32), and the fact that $\boldsymbol{L}_n^{jH}\overline{\boldsymbol{h}}_k^j = \boldsymbol{0}$.

Since the blind estimate of $\overline{\boldsymbol{h}}_k^j$ discussed in Section III always has an arbitrary phase ambiguity, the data bits must be differentially encoded and decoded, i.e., the receiver detects $\beta_k[i] \triangleq b_k[i]b_k[i-1]$. In order to make use of the received signal at both antennas, we use the following equal gain differential combining rule for detecting $\beta_k[i]$

$$\hat{\beta}_k[i] = \mathrm{sgn}\{\Re[(\boldsymbol{m}_k^{1H}\boldsymbol{r}^1[i])(\boldsymbol{m}_k^{1H}\boldsymbol{r}^1[i-1])^* + (\boldsymbol{m}_k^{2H}\boldsymbol{r}^2[i])(\boldsymbol{m}_k^{2H}\boldsymbol{r}^2[i-1])^*]\}. \tag{41}$$

Finally, the blind linear MMSE multiuser detection algorithms in white and correlated noise are summarized in Table I. The CCD-based method is based on the fast algorithm for computing CCD in [28]. Min-eigenvector (**a** denotes the eigenvector corresponding to the minimum eigenvalue of the matrix **A**.

TABLE I

SUMMARY OF SUBSPACE BLIND LINEAR MMSE MULTIUSER DETECTION ALGORITHMS IN WHITE AND CORRELATED NOISE

Detector in white noise:		
$\mathbf{X}$	$\triangleq$	$[\mathbf{r}[0]\ \mathbf{r}[1]\ \cdots\ \mathbf{r}[M-1]]$
1. Compute sample autocorrelation		
$\mathbf{R}$	$=$	$\frac{1}{M}\mathbf{X}\mathbf{X}^H$
2. Compute eigendecomposition		
$\mathbf{R}$	$=$	$\mathbf{U}_s\mathbf{\Lambda}_s\mathbf{U}_s^H + \sigma^2\mathbf{U}_n\mathbf{U}_n^H$
3. Estimate channel		
$\bar{\mathbf{g}}_k$	$=$	min-eigenvector $\left(\overline{\mathbf{C}}_k^T\mathbf{U}_n\mathbf{U}_n^H\overline{\mathbf{C}}_k\right)$
$\bar{\mathbf{h}}_k$	$=$	$\overline{\mathbf{C}}_k\bar{\mathbf{g}}_k$
4. Form detector		
$\mathbf{m}_k$	$=$	$\mathbf{U}_s\mathbf{\Lambda}_s^{-1}\mathbf{U}_s^H\bar{\mathbf{h}}_k$
Detector in correlated noise:		
$\mathbf{X}_j$	$\triangleq$	$[\mathbf{r}^j[0]\ \mathbf{r}^j[1]\ \cdots\ \mathbf{r}^j[M-1]]$, $j=1,2$
1. Compute QR and SVD		
$\frac{1}{\sqrt{M}}\mathbf{X}_j^H$	$=$	$\mathbf{Q}_j\mathbf{\Upsilon}_j$, $j=1,2$
$\mathbf{Q}_1^H\mathbf{Q}_2$	$=$	$\mathbf{V}_1\mathbf{\Gamma}\mathbf{V}_2^H$
2. Compute noise subspaces		
$\mathbf{L}^j$	$=$	$\mathbf{\Upsilon}_j^{-1}\mathbf{V}_j = [\mathbf{L}_s^j\ \mathbf{L}_n^j]$, $j=1,2$
3. Estimate channels		
$\bar{\mathbf{g}}_k^j$	$=$	min-eigenvector $\left(\overline{\mathbf{C}}_k^T\mathbf{L}_n^j\mathbf{L}_n^{jH}\overline{\mathbf{C}}_k\right)$
$\bar{\mathbf{h}}_k^j$	$=$	$\overline{\mathbf{C}}_k\bar{\mathbf{g}}_k^j$, $j=1,2$
4. Form detectors		
$\mathbf{m}_k^j$	$=$	$\mathbf{L}_s^j\mathbf{L}_s^{jH}\bar{\mathbf{h}}_k^j$, $j=1,2$

V. GROUP-BLIND LINEAR MULTIUSER DETECTORS

The blind linear detectors discussed in the Section IV are based on the assumption that the receiver knows only the spreading sequence of the given user. In the CDMA uplink, however, the receiver typically knows the spreading sequences of a group of users, e.g., users within the same cell. It is natural to expect that some performance gains can be achieved if the knowledge of other users' spreading sequences can be exploited in detecting each individual user's data. In this section, we develop such techniques. In what follows it is assumed that the receiver has the knowledge of the first $\tilde{K}(\tilde{K} \leq K)$ users' spreading sequences, whereas the spreading sequences of the rest $(K - \tilde{K})$ users are unknown to the receiver. Denote $\tilde{\boldsymbol{H}}$ as the $(Pm \times \tilde{r})$ matrix consisting of the first $\tilde{r}$ columns of $\boldsymbol{H}$, where $\tilde{r} \triangleq \tilde{K}(m + \iota)$ denotes the dimension of the subspace of the known users. It is assumed that $\tilde{\boldsymbol{H}}$ has full column rank $\tilde{r}$. [Recall that it is also assumed that $\boldsymbol{H}$ has full column rank $r \triangleq K(m + \iota)$].

A. Group-Blind Linear Detectors in White Noise

The basic idea behind the group-blind detectors is to suppress the interference from the known users based on the spreading sequences of these users and to suppress the interference from other unknown users using subspace-based blind methods. We first consider the zero-forcing detector $\boldsymbol{d}_k$ given by (36), which eliminates MAI and ISI completely, at the expense of enhancing the noise level. In order to facilitate the derivation of its group-blind form, we need the following alternative definition of this detector.

Definition 1 (Group-Blind Linear Zero-Forcing Detector): The group-blind linear zero-forcing detector for user $k(1 \leq k \leq \tilde{K})$ is given by the solution to the following constrained optimization problem:

$$\overline{\boldsymbol{d}}_k = \arg \min_{\boldsymbol{d} \in \mathrm{range}(\boldsymbol{H})} |\boldsymbol{d}^H \boldsymbol{H}|^2 \quad \text{subject to } \boldsymbol{d}^H\tilde{\boldsymbol{H}} = \boldsymbol{1}_{\tilde{K}\iota+k}^T. \tag{42}$$

In the Appendix, it is shown that $\bar{\boldsymbol{d}}_k = \boldsymbol{d}_k$. The second group-blind detector considered is a hybrid detector which zero-forces the interference caused by the $\tilde{K}$ known users and suppresses the interference from unknown users according to the MMSE criterion.

Definition 2 (Group-Blind Linear Hybrid Detector): The group-blind linear hybrid detector for user $k(1 \leq k \leq \tilde{K})$ is given by the solution to the following constrained optimization problem:

$$\overline{\boldsymbol{w}}_k = \arg \min_{\boldsymbol{w} \in \text{range}(\tilde{\boldsymbol{H}})} E\{|b_k[i] - \boldsymbol{w}_k^H \boldsymbol{r}[i]|^2\}, \quad \text{subject to } \boldsymbol{w}^H \tilde{\boldsymbol{H}} = \boldsymbol{1}_{\tilde{K}\iota+k}^T. \tag{43}$$

Define the projection matrices

$$\tilde{\boldsymbol{P}} \stackrel{\Delta}{=} \tilde{\boldsymbol{H}}(\tilde{\boldsymbol{H}}^H \tilde{\boldsymbol{H}})^{-1}\tilde{\boldsymbol{H}}^H, \quad \text{and} \quad \breve{\boldsymbol{P}} \stackrel{\Delta}{=} \boldsymbol{I}_{Pm} - \tilde{\boldsymbol{P}}. \tag{44}$$

Hence, $\tilde{\boldsymbol{P}}$ projects any signal onto the subspace range$(\tilde{\boldsymbol{H}})$, whereas $\breve{\boldsymbol{P}}$ projects any signal onto the subspace null$(\tilde{\boldsymbol{H}}^T)$. It is then easily seen that the matrix $(\breve{\boldsymbol{P}}\boldsymbol{R}\breve{\boldsymbol{P}})$ has an eigenstructure of the form

$$\breve{\boldsymbol{P}}\boldsymbol{R}\breve{\boldsymbol{P}} = [\breve{\boldsymbol{U}}_s \quad \breve{\boldsymbol{U}}_n \quad \breve{\boldsymbol{U}}_o] \begin{bmatrix} \breve{\boldsymbol{\Lambda}}_s & \boldsymbol{0} & \boldsymbol{0} \\ \boldsymbol{0} & \sigma^2 \boldsymbol{I}_{Pm-r} & \boldsymbol{0} \\ \boldsymbol{0} & \boldsymbol{0} & \boldsymbol{0} \end{bmatrix} \cdot \begin{bmatrix} \breve{\boldsymbol{U}}_s^H \\ \breve{\boldsymbol{U}}_n^H \\ \breve{\boldsymbol{U}}_o^H \end{bmatrix} \tag{45}$$

where $\breve{\boldsymbol{\Lambda}}_s = \text{diag}(\breve{\lambda}_1, \cdots, \breve{\lambda}_{r-\tilde{r}})$, with $\breve{\lambda}_i > \sigma^2, i = 1, \cdots, r - \tilde{r}$; and the columns of $\breve{\boldsymbol{U}}_s$ form an orthonormal basis of the subspace range$(\boldsymbol{H}) \cap$ null$(\tilde{\boldsymbol{H}}^T)$. We next define a group-blind MMSE detector. As noted in Section IV, any linear detector must lie in range$(\boldsymbol{H}) =$ range$(\tilde{\boldsymbol{H}}) +$ range$(\breve{\boldsymbol{U}}_s)$. The group-blind MMSE detector has the form $\overline{\boldsymbol{m}}_k = \tilde{\boldsymbol{m}}_k + \breve{\boldsymbol{m}}_k$, where $\tilde{\boldsymbol{m}}_k \in$ range$(\tilde{\boldsymbol{H}})$ and $\breve{\boldsymbol{m}}_k \in$ range$(\breve{\boldsymbol{U}}_s)$, such that $\tilde{\boldsymbol{m}}_k$ suppresses the interference from the known users in the MMSE sense, and $\breve{\boldsymbol{m}}_k$ suppresses the interference from the unknown users in the MMSE sense. Formally, we have the following definition. Denote $\tilde{\boldsymbol{b}}[i]$ as the vector consisting of the first $\tilde{K}$ elements of $\boldsymbol{b}[i]$.

Definition 3 (Group-Blind Linear MMSE Detector): Let $\tilde{\boldsymbol{r}}[i] = \tilde{\boldsymbol{H}}\tilde{\boldsymbol{b}}[i] + \boldsymbol{v}[i]$ be the components of the received signal $\boldsymbol{r}[i]$ in (12) consisting of the signals from the known users plus the noise. The group-blind linear MMSE detector for user $k(1 \leq k \leq \tilde{K})$ is given by $\overline{\boldsymbol{m}}_k = \tilde{\boldsymbol{m}}_k + \breve{\boldsymbol{m}}_k$, where $\tilde{\boldsymbol{m}}_k \in \tilde{\boldsymbol{H}}$ and $\breve{\boldsymbol{m}}_k \in \breve{\boldsymbol{U}}_s$, such that

$$\tilde{\boldsymbol{m}}_k = \arg \min_{\boldsymbol{m} \in \text{range}(\tilde{\boldsymbol{H}})} E\{|b_k[i] - \boldsymbol{m}^H \tilde{\boldsymbol{r}}[i]|^2\} \tag{46}$$

$$\breve{\boldsymbol{m}}_k = \arg \min_{\boldsymbol{m} \in \text{range}(\breve{\boldsymbol{U}}_s)} E\{|b_k[i] - (\boldsymbol{m} + \tilde{\boldsymbol{m}}_k)^H \boldsymbol{r}[i]|^2\}. \tag{47}$$

Note that in general, $\overline{\boldsymbol{m}}_k$ is different from the linear MMSE detector $\boldsymbol{m}_k$ defined in (37).

The following results give expressions for the three group-blind linear detectors defined above in terms of the known users' channel matrix $\tilde{\boldsymbol{H}}$ and the known-user signal subspace components $\breve{\boldsymbol{\Lambda}}_s$ and $\breve{\boldsymbol{U}}_s$ defined in (45). The proofs of these results are found in the Appendix.

Proposition 1 (Group-Blind Linear Zero-Forcing Detector—Form I): The group-blind linear zero-forcing detector for the kth user is given by

$$\bar{\boldsymbol{d}}_k = [\boldsymbol{I}_{Pm} - \breve{\boldsymbol{U}}_s(\breve{\boldsymbol{\Lambda}}_s - \sigma^2 \boldsymbol{I}_{r-\tilde{r}})^{-1}\breve{\boldsymbol{U}}_s^H \boldsymbol{R}]\tilde{\boldsymbol{H}}(\tilde{\boldsymbol{H}}^H \tilde{\boldsymbol{H}})^{-1}\boldsymbol{1}_{\tilde{K}\iota+k}, \quad k = 1, \ldots, \tilde{K}. \tag{48}$$

Proposition 2 (Group-Blind Linear Hybrid Detector—Form I): The group-blind linear hybrid detector for the kth user is given by

$$\overline{\boldsymbol{w}}_k = (\boldsymbol{I}_{Pm} - \breve{\boldsymbol{U}}_s \breve{\boldsymbol{\Lambda}}_s^{-1} \breve{\boldsymbol{U}}_s^H \boldsymbol{R})\tilde{\boldsymbol{H}}(\tilde{\boldsymbol{H}}^H \tilde{\boldsymbol{H}})^{-1}\boldsymbol{1}_{\tilde{K}\iota+k}, \quad k = 1, \ldots, \tilde{K}. \tag{49}$$

Proposition 3 (Group-Blind Linear MMSE Detector—Form I): The group-blind linear MMSE detector for the kth user is given by

$$\overline{\boldsymbol{m}}_k = (\boldsymbol{I}_{Pm} - \breve{\boldsymbol{U}}_s \breve{\boldsymbol{\Lambda}}_s^{-1} \breve{\boldsymbol{U}}_s^H \boldsymbol{R})\tilde{\boldsymbol{H}}(\tilde{\boldsymbol{H}}^H \tilde{\boldsymbol{H}} + \sigma^2 \boldsymbol{I}_{\tilde{r}})^{-1}\boldsymbol{1}_{\tilde{K}\iota+k}, \quad k = 1, \ldots, \tilde{K}. \tag{50}$$

In the above results, the group-blind detectors are expressed in terms of the known-user signal subspace components $\breve{\boldsymbol{\Lambda}}_s$ and $\breve{\boldsymbol{U}}_s$ defined in (45). Alternatively, they can be expressed in terms of the signal subspace components $\boldsymbol{\Lambda}_s$ and $\boldsymbol{U}_s$ of all users defined in (22), as given by the following three results. Their proofs are also given in the Appendix.

Proposition 4 (Group-Blind Linear Zero-Forcing Detector—Form II): The group-blind linear zero-forcing detector for the kth user is given by

$$\bar{\boldsymbol{d}}_k = \boldsymbol{U}_s(\boldsymbol{\Lambda}_s - \sigma^2 \boldsymbol{I}_r)^{-1}\boldsymbol{U}_s^H \tilde{\boldsymbol{H}} \cdot [\tilde{\boldsymbol{H}}^H \boldsymbol{U}_s(\boldsymbol{\Lambda}_s - \sigma^2 \boldsymbol{I}_r)\boldsymbol{U}_s \tilde{\boldsymbol{H}}]^{-1}\boldsymbol{1}_{\tilde{K}\iota+k}, \quad k = 1, \ldots, \tilde{K}. \tag{51}$$

Proposition 5 (Group-Blind Linear Hybrid Detector—Form II): The group-blind linear hybrid detector for the kth user is given by

$$\overline{\boldsymbol{w}}_k = \boldsymbol{U}_s \boldsymbol{\Lambda}_s^{-1} \boldsymbol{U}_s^H \tilde{\boldsymbol{H}}[\tilde{\boldsymbol{H}}^H \boldsymbol{U}_s \boldsymbol{\Lambda}_s^{-1} \boldsymbol{U}_s^H \tilde{\boldsymbol{H}}]^{-1}\boldsymbol{1}_{\tilde{K}\iota+k}, \quad k = 1, \ldots, \tilde{K}. \tag{52}$$

In order to form the group-blind linear MMSE detector in terms of the subspace $\boldsymbol{U}_s$, we need to first find a basis for the subspace range$(\breve{\boldsymbol{U}}_s)$. Clearly, range$(\breve{\boldsymbol{P}}\boldsymbol{U}_s) =$ range$(\breve{\boldsymbol{U}}_s)$. Consider the (rank-deficient) QR factorization of the $(Pm \times r)$ matrix $(\breve{\boldsymbol{P}}\boldsymbol{U}_s)$

$$\breve{\boldsymbol{P}}\boldsymbol{U}_s = [\boldsymbol{Q}_s \quad \boldsymbol{Q}_o] \begin{bmatrix} \boldsymbol{R}_s & \boldsymbol{R}_o \\ \boldsymbol{0} & \boldsymbol{0} \end{bmatrix} \boldsymbol{\Pi} \tag{53}$$

where $\boldsymbol{Q}_s$ is a $(Pm \times \tilde{r})$ matrix, $\boldsymbol{R}_s$ is a $(\tilde{r} \times \tilde{r})$ nonsingular upper triangular matrix, and $\boldsymbol{\Pi}$ is a permutation matrix. Then the columns of $\boldsymbol{Q}_s$ forms an orthonormal basis of range$(\breve{\boldsymbol{U}}_s)$.

Proposition 6 (Group-Blind Linear MMSE Detector—Form II): The group-blind linear MMSE detector for the kth user is given by

$$\begin{aligned}\overline{\boldsymbol{m}}_k = &[\boldsymbol{I}_{Pm} - (\boldsymbol{Q}_s\boldsymbol{R}_s^{-H})(\boldsymbol{\Pi}\boldsymbol{\Lambda}_s\boldsymbol{\Pi}^T)^{-1}(\boldsymbol{Q}_s\boldsymbol{R}_s^{-H})^H\boldsymbol{R}] \\ &\cdot \tilde{\boldsymbol{H}}(\tilde{\boldsymbol{H}}^H\tilde{\boldsymbol{H}} + \sigma^2\boldsymbol{I}_{\tilde{r}})^{-1}\mathbf{1}_{\tilde{K}\iota+k}, \\ &k = 1, \ldots, \tilde{K}.\end{aligned} \tag{54}$$

It is seen that the form-I group-blind detectors are based on the estimate of the signal subspace of the matrix $(\breve{\boldsymbol{P}}\boldsymbol{R}\breve{\boldsymbol{P}})$, whereas the form-II group-blind detectors are based on the estimate of the signal subspace of the matrix $\boldsymbol{R}$. Since the signal subspace dimension $(r - \tilde{r})$ of $(\breve{\boldsymbol{P}}\boldsymbol{R}\breve{\boldsymbol{P}})$ is less than that of $\boldsymbol{R}$, which is r, the form-I implementations in general give a more accurate estimation of the group-blind detectors. On the other hand, as discussed in Section III, the estimation of the given users' channels (in order to form $\tilde{\boldsymbol{H}}$) is based on the eigendecomposition of $\boldsymbol{R}$. Hence, the form-II group-blind detectors are more efficient in terms of implementations, since they do not require the eigendecomposition (45), which is required by the form-I group-blind detectors. If, however, the user channels are estimated by some other means not involving the eigendecomposition of $\boldsymbol{R}$, then the form-I detectors can be computationally less complex than the form-II detectors, since the dimension of the estimated signal subspace of the former is less than that of the latter. (That is, of course, if the computationally efficient subspace tracking algorithms [4], instead of the conventional eigendecomposition, are used.) The performance of the above detectors is assessed through simulations in Section VI.

Remark 2: In both the group-blind zero-forcing detector and the group-blind hybrid detector, the interfering signals from known users are nulled out by a projection of the received signal onto the orthogonal subspace of these users' signal subspace. The unknown interfering users' signals are then suppressed by identifying the subspace spanned by these users, followed by a linear transformation in this subspace based on the zero-forcing or the MMSE criterion. In the group-blind MMSE detector, the interfering users from the known and the unknown users are suppressed separately under the MMSE criterion. The suppression of the unknown users again relies upon the identification of the signal subspace spanned by these users.

B. Group-Blind Linear Detectors in Correlated Noise

We next consider the group-blind linear detector in correlated ambient noise based on the CCD method discussed in Section III-C. Similar to the case of white noise, let $\tilde{\boldsymbol{H}}^j, j = 1, 2$ be the channel matrix of the known users at antenna j. Since the signal subspace cannot be directly identified in the CCD, we will not consider the group-blind linear zero-forcing or MMSE detectors, which require the identification of some signal subspace. Nevertheless, the form-II group-blind linear hybrid detector can be easily constructed for correlated noise, as given by the following result. The proof is found in the Appendix.

TABLE II
SUMMARY OF SUBSPACE GROUP-BLIND LINEAR HYBRID MULTIUSER DETECTION ALGORITHMS (FORM-II) IN WHITE AND CORRELATED NOISE

	Detector in white noise:
	$\mathbf{X} \triangleq [\mathbf{r}[0]\ \mathbf{r}[1] \cdots \mathbf{r}[M-1]]$
1.	Compute sample autocorrelation
	$\mathbf{R} = \frac{1}{M}\mathbf{X}\mathbf{X}^H$
2.	Compute eigendecomposition
	$\mathbf{R} = \mathbf{U}_s\mathbf{\Lambda}_s\mathbf{U}_s^H + \sigma^2\mathbf{U}_n\mathbf{U}_n^H$
3.	Estimate channels
	$\bar{\mathbf{g}}_k = \text{min eigenvector}\left(\overline{\mathbf{C}}_k^T\mathbf{U}_n\mathbf{U}_n^H\overline{\mathbf{C}}_k\right)$
	$\mathbf{h}_k = \overline{\mathbf{C}}_k\bar{\mathbf{g}}_k,\ k = 1, \cdots, \tilde{K}$
	form $\tilde{\mathbf{H}}$ using $\left(\mathbf{h}_1, \cdots, \mathbf{h}_{\tilde{K}}\right)$
4.	Form detector
	$\mathbf{w}_k = \mathbf{U}_s\mathbf{\Lambda}_s^{-1}\mathbf{U}_s^H\tilde{\mathbf{H}}\left[\tilde{\mathbf{H}}^H\mathbf{U}_s\mathbf{\Lambda}_s^{-1}\mathbf{U}_s^H\tilde{\mathbf{H}}\right]^{-1}\mathbf{1}_{\tilde{K}\iota+k},$ $k = 1, \cdots, \tilde{K}$
	Detector in correlated noise:
	$\mathbf{X}_j \triangleq [\mathbf{r}^j[0]\ \mathbf{r}^j[1] \cdots \mathbf{r}^j[M-1]],\ j = 1, 2$
1.	Compute QR and SVD
	$\frac{1}{\sqrt{M}}\mathbf{X}_j^H = \mathbf{Q}_j\mathbf{\Upsilon}_j,\ j = 1, 2$
	$\mathbf{Q}_1^H\mathbf{Q}_2 = \mathbf{V}_1\mathbf{\Gamma}\mathbf{V}_2^H$
2.	Compute noise subspaces
	$\mathbf{L}^j = \mathbf{\Upsilon}_j^{-1}\mathbf{V}_j = [\mathbf{L}_s^j\ \mathbf{L}_n^j],\ j = 1, 2$
3.	Estimate channels
	$\bar{\mathbf{g}}_k^j = \text{min–eigenvector}\left(\overline{\mathbf{C}}_k^T\mathbf{L}_n^j\mathbf{L}_n^{jH}\overline{\mathbf{C}}_k\right)$
	$\bar{\mathbf{h}}_k^j = \overline{\mathbf{C}}_k\bar{\mathbf{g}}_k^j,\ j = 1, 2$
	form $\tilde{\mathbf{H}}^j$ using $\left(\bar{\mathbf{h}}_1^j, \cdots, \bar{\mathbf{h}}_{\tilde{K}}^j\right)$
4.	Form detectors
	$\mathbf{w}_k^j = \mathbf{L}_s^j\mathbf{L}_s^{jH}\tilde{\mathbf{H}}^j\left(\tilde{\mathbf{H}}^{jH}\mathbf{L}_s^j\mathbf{L}_s^{jH}\tilde{\mathbf{H}}^j\right)^{-1}\mathbf{1}_{\tilde{K}\iota+k},$ $j = 1, 2;\ k = 1, \cdots, \tilde{K}$

Proposition 7 (Group-Blind Hybrid Detector for Correlated Noise—Form II): The hybrid detector for the kth user at the jth antenna in correlated noise is given by

$$\begin{aligned}\overline{\boldsymbol{w}}_k^j = &\boldsymbol{L}_s^j\boldsymbol{L}_s^{jH}\tilde{\boldsymbol{H}}^j(\tilde{\boldsymbol{H}}^{jH}\boldsymbol{L}_s^j\boldsymbol{L}_s^{jH}\tilde{\boldsymbol{H}}^j)^{-1}\mathbf{1}_{\tilde{K}\iota+k}, \\ &j = 1, 2; \quad k = 1, \ldots, \tilde{K}\end{aligned} \tag{55}$$

where $\boldsymbol{L}_s^j$ is defined in (32).

Again, the equal gain differential combining rule (41) (with $\boldsymbol{m}_k^j$ replaced by $\overline{\boldsymbol{w}}_k^j$) is employed to detect the differential bit $\beta_k[i]$. Finally, the form-II group-blind linear hybrid detectors in both white and correlated noise are summarized in Table II.

Remark 3: Comparing Tables I and II, it is seen that the first three steps involved in computing the blind detector and the group-blind detectors are exactly the same. (Note that here a CDMA uplink scenario is considered and the detectors for all the $\tilde{K}$ users in the cell are computed.) In the fourth step, however, the group-blind detector involves computing an extra matrix inversion (cf. Step 4 in Fig. 2). Since the dominant computation in both the blind detector and the group-blind detector is the eigendecomposition in Steps 2 and 3, the group-blind detector introduces little attendant increase in computational complexity.

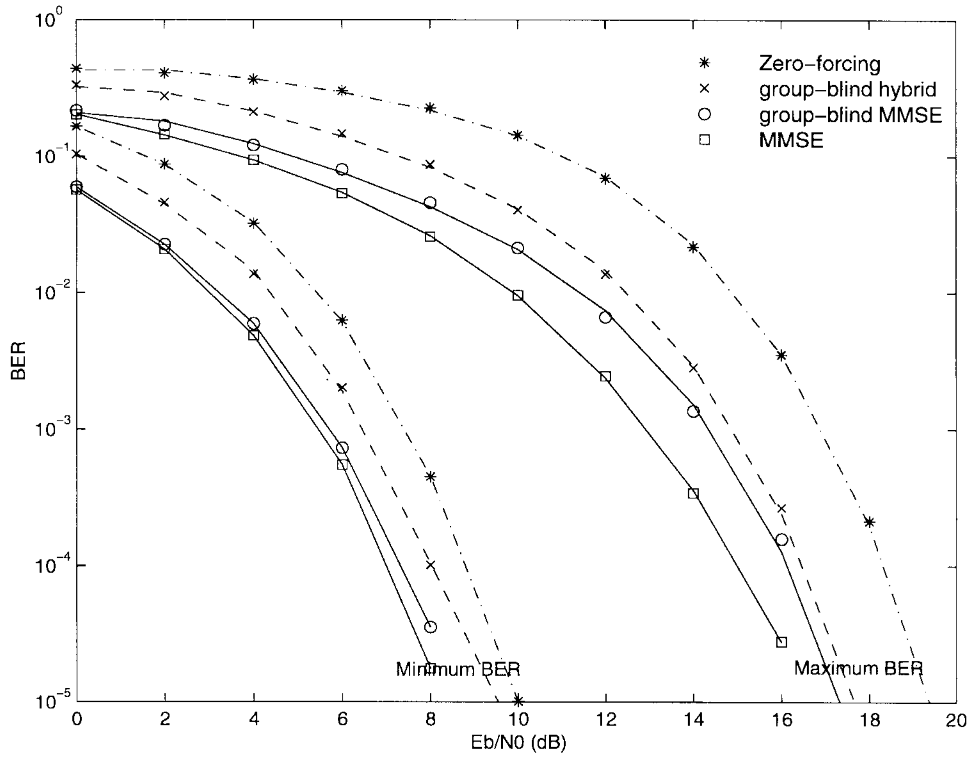

Fig. 1. Comparision of the performance of four exact linear detectors in white noise. $K = 10, \tilde{K} = 7$.

VI. Simulation Examples

In this section, we provide computer simulation results to demonstrate the performance of the proposed blind and group-blind linear multiuser detectors under a number of channel conditions. The simulated system is an asynchronous CDMA system with processing gain $N = 15$. The m-sequences of length 15 and their shifted versions are employed as the user spreading sequences. The chip pulse is a raised cosine pulse with roll-off factor 0.5. The initial delay d_k of each user is uniform on $[0, 4T_c]$. Each user's channel has $L = 3$ paths. The delay of each path $\tau_{k,l}$ is uniform on $[0, 6T_c]$. Hence, the maximum delay spread is one symbol interval, i.e., $\iota = 1$. The fading gain of each path in each user's channel is generated from a complex Gaussian distribution and fixed for all simulations. The path gains in each user's channel are normalized so that each user's signal arrives at the receiver with the same power. The over sampling factor is $p = 2$. The smoothing factor is $m = 2$. Hence, this system can accommodate up to $\lceil (m+\iota)/(m-\iota) \cdot P \rceil = 10$ users. The number of users in the simulation is ten, with seven known users, i.e., $K = 10$ and $\tilde{K} = 7$. The length of each user's signal frame is $M = 200$.

In each simulation, an eigendecomposition is performed on the sample autocorrelation matrix of the received signals. The signal subspace consists of the eigenvectors corresponding to the r largest eigenvalues. (Recall that $r \triangleq K(m + \iota)$ is the dimension of the signal subspace.) The rest eigenvectors constitute the noise subspace. An estimate of the noise variance σ^2 is given by the average of the $(Pm - r)$ smallest eigenvalues. For algorithmic details of the matrix operations involved in computing the various detectors, see [5].

A. Receiver Performance in White Noise

We first compare the performance of four exact detectors (i.e., assuming that $\boldsymbol{H}$ and σ^2 are known), namely:

1) the linear MMSE detector $\boldsymbol{m}_k$ in (37);
2) the linear zero-forcing detector $\boldsymbol{d}_k$ in (36) [or equivalently, the group-blind linear zero-forcing detector $\overline{\boldsymbol{d}}_k$ in (42), since $\boldsymbol{d}_k = \overline{\boldsymbol{d}}_k$];
3) the group-blind linear hybrid detector $\overline{\boldsymbol{w}}_k$ in (43);
4) the group-blind linear MMSE detector $\overline{\boldsymbol{m}}_k$ in (46) and (47).

For each of these detectors and for each value of (E_b/N_o), the minimum and the maximum BER among the seven known users is plotted in Fig. 1. It is seen from this figure that, as expected, the closer the detector is to the true linear MMSE detector, the better its performance is.

Next the performance of the various estimated group-blind detectors (i.e., the detectors are estimated based on the M received signal vectors) is shown in Fig. 2. It is seen that at low (E_b/N_o), the group-blind MMSE detectors perform the best; whereas at high (E_b/N_o), the group-blind hybrid detectors perform the best. This is because the hybrid detector zero-forces the known users' signals and it enhances the noise level, whereas the group-blind linear MMSE detector suppresses both the interference and the noise. At high (E_b/N_o), the group-blind hybrid and group-blind MMSE detectors tend to become the same. However, the implementation of the latter requires the estimate of the noise level. When the noise level is low, the estimate is noisy, which consequently deteriorates the performance of the group-blind MMSE detector. It is also seen that the performance of the form-I detectors is only slightly

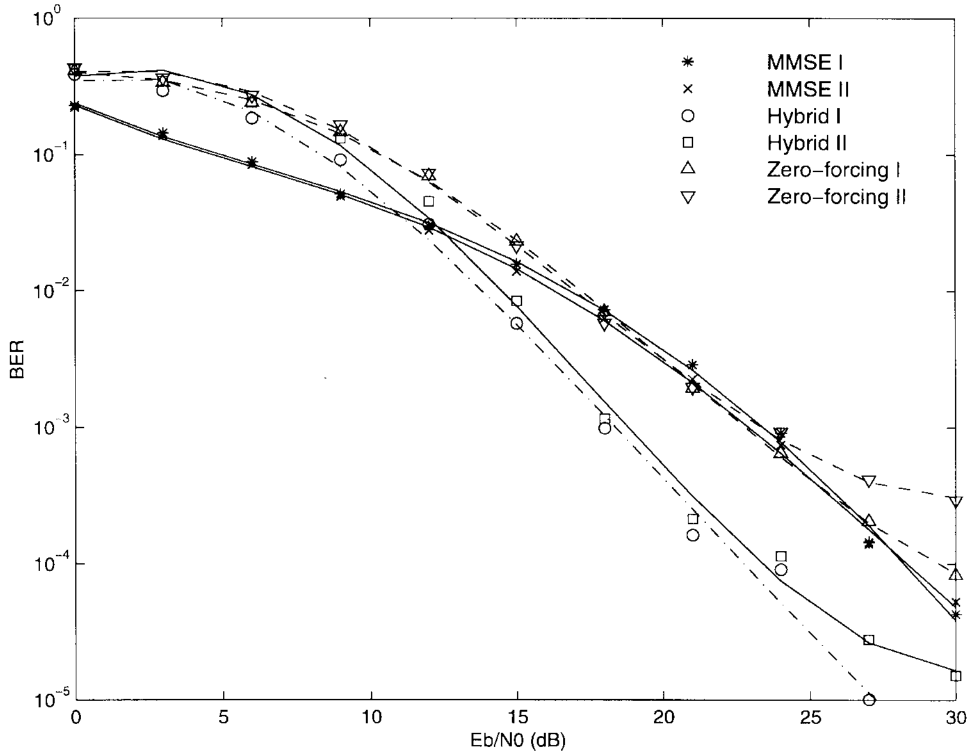

(a)

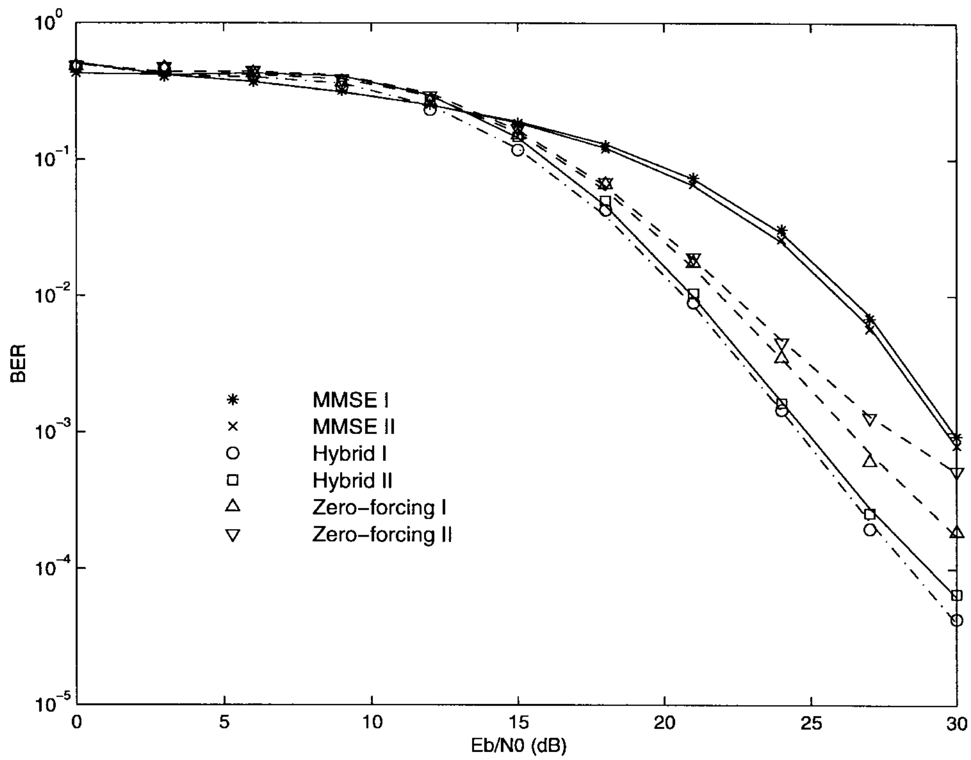

(b)

Fig. 2. Comparison of the performance of various *estimated* group-blind detectors in white noise. $K = 10, \tilde{K} = 7$. (a) Minimun BER. (b) Maximum BER.

better than the corresponding form-II detectors, at the expense of higher computational complexity.

Comparing Figs. 1 and 2, it is seen that the performance of the estimated detectors is of substantial distance from that of the corresponding exact detectors, for the block size considered here (i.e., $M = 200$). It is known that the subspace detectors converge to the exact detectors at a rate of $O(\sqrt{\log \log M/M})$ [25]. It is also seen from Fig. 2 that

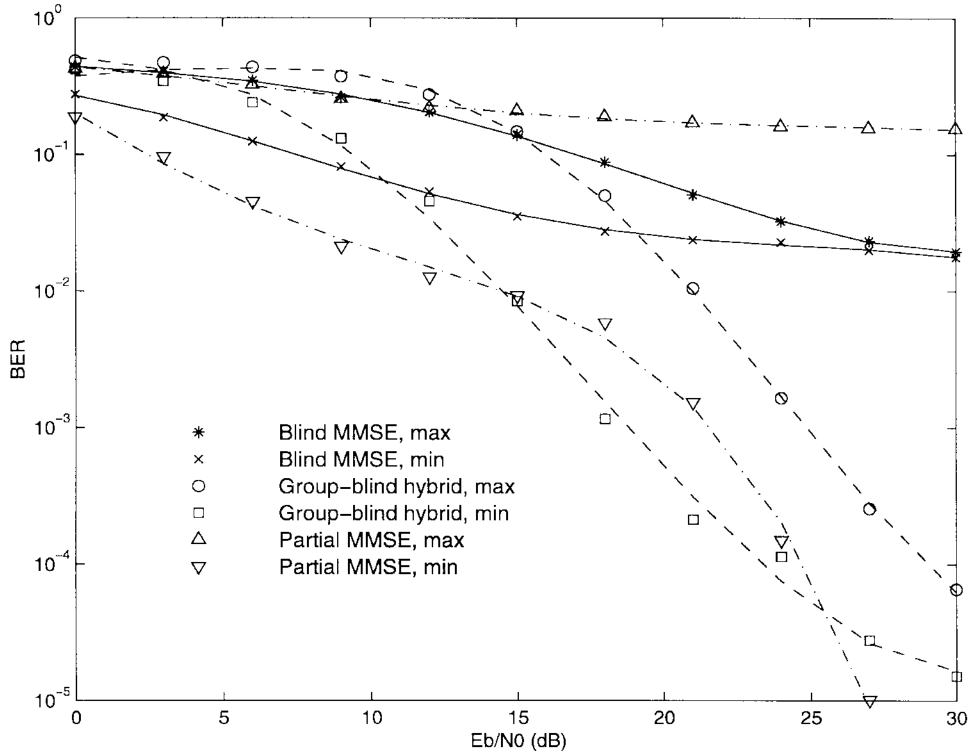

Fig. 3. Comparison of the performance of the blind and the group-blind linear detectors in white noise. $K = 10, \tilde{K} = 7$.

the form-II hybrid detector performs very well compared with other forms of group-blind detectors, even though it has the lowest computational complexity. Hence, in the subsequent simulation studies, we will compare the performance of the form-II hybrid detector with some previously proposed multiuser detectors.

We next compare the performance of the group-blind hybrid detector with that of the blind detector for the same system. The result is shown in Fig. 3, where the BER curves for the blind linear MMSE detector given by (39), the form-II group-blind linear hybrid detector given by (52), and a partial MMSE detector are plotted. The partial MMSE detector ignores the unknown users and forms the linear MMSE detector for the $\tilde{K}$ known users using the estimated matrix $\tilde{\boldsymbol{H}}$. It is seen that the group-blind detector significantly outperforms the blind MMSE detector and the partial MMSE detector. Indeed, the blind MMSE detector exhibits an error floor at high (E_b/N_o) values. This is due to the finite length of received signal frame, based on which the detector is estimated. The group-blind hybrid MMSE detector does not show an error floor in the BER range considered here. Of course, due to the finite signal frame length, the group-blind detector also has an error floor. But such a floor is much lower than that of the blind linear MMSE detector.

b. *Receiver Performance in Correlated Noise*

Next, we consider the performance of the blind and the group-blind linear detectors in correlated noise. The noise at each antenna j is modeled by an second order autoregressive (AR) model with coefficients $[a_1^j, a_2^j]$, i.e., the noise field is generated according to

$$v^j[n] = a_1^j\, v^j[n-1] + a_2^j\, v^j[n-2] + w^j[n],\ j = 1, 2 \quad (56)$$

where $v^j[n]$ is the noise sample at antenna j and sample n and $w^j[n]$ is a complex white Gaussian noise sample. The AR coefficients at the two antennas are chosen as $[a_1^1, a_2^1] = [1, -0.2]$ and $[a_1^2, a_2^2] = [1.2, -0.3]$. The performance of the group-blind linear hybrid detector given in Table II is compared with that of the blind linear MMSE detector given in Table I. The result is shown in Fig. 4. It is seen that similar to the white noise case, the proposed group-blind linear detector offers substantial performance gain over the blind linear detector.

Remark 4: Theoretically, both the blind detector and the group-blind detector converge to the true linear MMSE detector (at high signal-to-noise ratio) as the signal frame size $M \rightarrow \infty$. Hence, the asymptotic performance of the two detectors is the same at high signal-to-noise ratio (SNR). However, for a finite frame length M, the group-blind detector performs significantly better than the blind detector, as seen from the earlier simulation results. An intuitive explanation for such performance improvement is that more information about the multiuser environment is incorporated in forming the group-blind detector. For example, consider the two detectors in white noise summarized in Tables I and II. The computation for subspace decomposition and channel estimation involved in the two detectors is exactly the same (cf. Steps 1–3 in Tables I and II). However, the blind detector is formed based solely on the composite channel of the desired user (cf. Step 4 in Table I); where as the group-blind detector is formed based on the composite channels of all known users (cf. Step 4

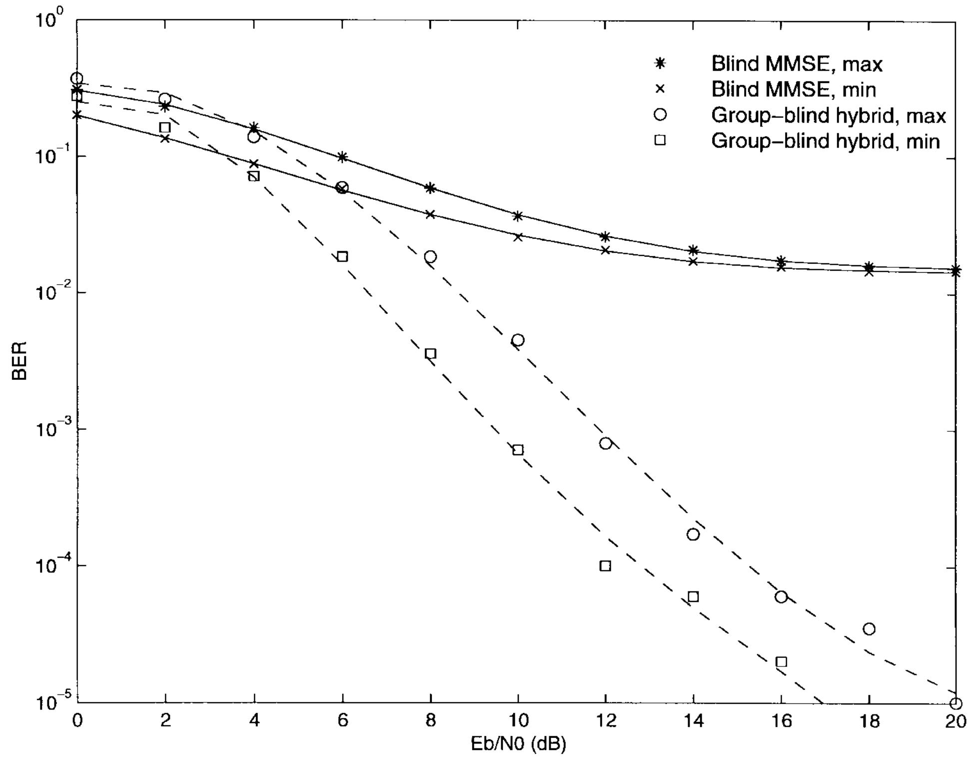

Fig. 4. Comparison of the performance of the blind and group-blind linear detectors in correlated noise. $K = 10, \tilde{K} = 7$.

in Table II). By incorporating more information about the multiuser channel, the estimated group-blind detector is more accurate than the estimated blind detector, i.e., the former is "closer" to the exact detector than the latter. Of course, an analytical performance comparison between the group-blind detector and the blind detector under finite sample size is of particular interest and will be investigated in the future.

Remark 5: It is seen from Fig. 1 that when the spreading waveforms and the channels of all users are known, all three forms of the exact group-blind detectors perform worse than the linear MMSE detector, which is the exact blind detector. This is because the zero-forcing and the hybrid group-blind detectors zero-force all or some users' signals and enhance the noise level, whereas the group-blind MMSE detector is defined in terms of a specific constrained form (cf. Definition 3), which in general is different from the true MMSE detector. However, with imperfect channel information, the roles are reversed and the group-blind detectors outperform the blind detector. Of course, both the blind and the group-blind detectors are developed based on the assumption that the multiuser channel is not perfectly known, and the study of the performance of the exact detectors is only of theoretical interest. Nevertheless, it is interesting to observe that by changing the assumption on the prior knowledge about the channel, the relative performance of two detectors can be different.

VII. Conclusions

In this paper, we have developed group-blind linear multiuser detection techniques for demodulating a group of given users in the uplink of a CDMA network. These new techniques make use of the spreading sequences and the estimated multipath channels of all known users to suppress the interference caused by users within the group and blindly suppress the interference caused by other unknown users. Several forms of group-blind linear detectors are defined based on different criteria, and their expressions are derived. Moreover, group-blind multiuser detection techniques in the presence of correlated noise have also been developed. It is seen that the form-II group-blind linear hybrid multiuser detectors (cf. Table II) in both white and correlated noise have low computational complexities and very good performance, making them the ideal candidates for implementation in practical systems. Simulation results have demonstrated that the proposed group-blind linear multiuser detection methods offer substantial performance gains over the blind linear multiuser detection techniques in a CDMA uplink environment, with little attendant increase in computational complexity. Some possible future directions of research on group-blind multiuser detection include analytical performance comparisons between the group-blind detectors and the blind detectors and sensitivity analysis of subspace rank mismatch on the detector performance.

Appendix

Proof of $\bar{\boldsymbol{d}}_k = \boldsymbol{d}_k$: We show that the group-blind linear zero-forcing detector defined in (42) is the same as the zero-forcing detector $\boldsymbol{d}_k$ defined in (36). First, because $\text{rank}(\boldsymbol{H}) = r$, the zero-forcing detector $\boldsymbol{d}_k$ in (36) is the unique signal $\boldsymbol{d} \in \text{range}(\boldsymbol{H})$, such that $\boldsymbol{d}^H \boldsymbol{H} = \boldsymbol{1}^T_{K\iota+k}$. Since $\tilde{\boldsymbol{H}}$ contains the first $\tilde{r}$ columns of $\boldsymbol{H}$, then

$$|\boldsymbol{d}^H \boldsymbol{H}|^2 = |\boldsymbol{d}^H \tilde{\boldsymbol{H}}|^2 + \sum_{l=\tilde{r}+1}^{Pm} |\boldsymbol{d}^H \boldsymbol{H}[:, l]|^2 \tag{57}$$

where $\boldsymbol{H}[:,l]$ denotes the lth column of $\boldsymbol{H}$, it then follows that for $\boldsymbol{d} \in \text{range}(\boldsymbol{H}), |\boldsymbol{d}^H\boldsymbol{H}|^2$ is minimized subject to $\boldsymbol{d}^H\tilde{\boldsymbol{H}} = \mathbf{1}^T_{\tilde{K}\iota+k}$, if and only if $\boldsymbol{d}^H\boldsymbol{H}[:,l] = 0$, for $l = \tilde{r}+1,\ldots,Pm$. That is, $\boldsymbol{d}^H\boldsymbol{H} = \mathbf{1}^T_{\tilde{K}\iota+k}$. Therefore, $\overline{\boldsymbol{d}}_k = \boldsymbol{d}_k$.

Proof of Proposition 1: Decompose $\overline{\boldsymbol{d}}_k$ into $\overline{\boldsymbol{d}}_k = \tilde{\boldsymbol{d}}_k + \breve{\boldsymbol{d}}_k$, where $\tilde{\boldsymbol{d}}_k \in \text{range}(\tilde{\boldsymbol{H}})$ and $\breve{\boldsymbol{d}}_k \in \text{range}(\breve{\boldsymbol{U}}_s)$. Substituting this into the constraint in (42), we have $\tilde{\boldsymbol{d}}_k = \tilde{\boldsymbol{H}}(\tilde{\boldsymbol{H}}^H\tilde{\boldsymbol{H}})^{-1}\mathbf{1}_{\tilde{K}\iota+k}$. Hence, the $\overline{\boldsymbol{d}}_k$ has the form of $\overline{\boldsymbol{d}}_k = \breve{\boldsymbol{U}}_s\boldsymbol{c}_k + \tilde{\boldsymbol{d}}_k$, for some $\boldsymbol{c}_k \in \mathcal{C}^{(r-\tilde{r})}$. Substituting this into the minimization problem in (42) we get

$$\begin{aligned}\boldsymbol{c}_k &= \arg\min_{\boldsymbol{c}\in\mathcal{C}^{(r-\tilde{r})}} E\{|(\breve{\boldsymbol{U}}_s\boldsymbol{c} + \tilde{\boldsymbol{w}}_k)^H\boldsymbol{H}|^2\}\\ &= \arg\min_{\boldsymbol{c}\in\mathcal{C}^{(r-\tilde{r})}} (\breve{\boldsymbol{U}}_s\boldsymbol{c}_k + \tilde{\boldsymbol{d}}_k)^H(\boldsymbol{R} - \sigma^2\boldsymbol{I}_{Pm})(\breve{\boldsymbol{U}}_s\boldsymbol{c}_k + \tilde{\boldsymbol{d}}_k)\\ &= -[\breve{\boldsymbol{U}}_s^H(\boldsymbol{R} - \sigma^2\boldsymbol{I}_{Pm})\breve{\boldsymbol{U}}_s]^{-1}\breve{\boldsymbol{U}}_s^H(\boldsymbol{R} - \sigma^2\boldsymbol{I}_{Pm})\tilde{\boldsymbol{d}}_k\\ &= -[\breve{\boldsymbol{U}}_s^H\breve{\boldsymbol{P}}(\boldsymbol{R} - \sigma^2\boldsymbol{I}_{Pm})\breve{\boldsymbol{P}}\breve{\boldsymbol{U}}_s]^{-1}\breve{\boldsymbol{U}}_s^H(\boldsymbol{R} - \sigma^2\boldsymbol{I}_{Pm})\tilde{\boldsymbol{d}}_k\\ &= -(\breve{\boldsymbol{\Lambda}}_s - \sigma^2\boldsymbol{I}_{r-\tilde{r}})^{-1}\breve{\boldsymbol{U}}_s^H(\boldsymbol{R} - \sigma^2\boldsymbol{I}_{Pm})\tilde{\boldsymbol{d}}_k\\ &= -(\breve{\boldsymbol{\Lambda}}_s - \sigma^2\boldsymbol{I}_{r-\tilde{r}})^{-1}\breve{\boldsymbol{U}}_s^H\boldsymbol{R}\tilde{\boldsymbol{d}}_k \end{aligned} \tag{58}$$

where the second equality follows from (22); the fourth equality follows from the facts that $\tilde{\boldsymbol{P}} + \breve{\boldsymbol{P}} = \boldsymbol{I}_{Pm}$ and $\breve{\boldsymbol{U}}_s^H\tilde{\boldsymbol{P}} = \mathbf{0}$, the fifth equality follows from (45), and the last equality follows from the fact that $\breve{\boldsymbol{U}}_s^H\tilde{\boldsymbol{d}}_k = \mathbf{0}$. Hence, $\overline{\boldsymbol{d}}_k = \breve{\boldsymbol{U}}_s\boldsymbol{c}_k + \tilde{\boldsymbol{d}}_k = [\boldsymbol{I}_{Pm} - (\breve{\boldsymbol{\Lambda}}_s - \sigma^2\boldsymbol{I}_{r-\tilde{r}})^{-1}\breve{\boldsymbol{U}}_s^H\boldsymbol{R}]\tilde{\boldsymbol{H}}(\tilde{\boldsymbol{H}}^H\tilde{\boldsymbol{H}})^{-1}\mathbf{1}_{\tilde{K}\iota+k}$.

Proof of Proposition 2: Decompose $\overline{\boldsymbol{w}}_k$ into $\overline{\boldsymbol{w}}_k = \tilde{\boldsymbol{w}}_k + \breve{\boldsymbol{w}}_k$, where $\tilde{\boldsymbol{w}}_k \in \text{range}(\tilde{\boldsymbol{H}})$ and $\breve{\boldsymbol{w}}_k \in \text{range}(\breve{\boldsymbol{U}}_s)$. Substituting this into the constraint in (43), we have $\tilde{\boldsymbol{w}}_k = \tilde{\boldsymbol{H}}(\tilde{\boldsymbol{H}}^H\tilde{\boldsymbol{H}})^{-1}\mathbf{1}_{\tilde{K}\iota+k}$. Hence, $\overline{\boldsymbol{w}}_k = \breve{\boldsymbol{U}}_s\boldsymbol{c}_k + \tilde{\boldsymbol{w}}_k$, for some $\boldsymbol{c}_k \in \mathcal{C}^{(r-\tilde{r})}$. Substituting this into the minimization problem in (43), we get

$$\begin{aligned}\boldsymbol{c}_k &= \arg\min_{\boldsymbol{c}\in\mathcal{C}^{(r-\tilde{r})}} E\{|b_k[i] - (\breve{\boldsymbol{U}}_s\boldsymbol{c} + \tilde{\boldsymbol{w}}_k)^H\boldsymbol{r}[i]|^2\}\\ &= \arg\min_{\boldsymbol{c}\in\mathcal{C}^{(r-\tilde{r})}} (\breve{\boldsymbol{U}}_s\boldsymbol{c} + \tilde{\boldsymbol{w}}_k)^H\boldsymbol{R}(\breve{\boldsymbol{U}}_s\boldsymbol{c} + \tilde{\boldsymbol{w}}_k)\\ &\quad - 2\Re\{\boldsymbol{c}^H\breve{\boldsymbol{U}}_s^H\overline{\boldsymbol{h}}_k\}\\ &= -(\breve{\boldsymbol{U}}_s^H\boldsymbol{R}\breve{\boldsymbol{U}}_s)^{-1}\breve{\boldsymbol{U}}_s^H\boldsymbol{R}\tilde{\boldsymbol{w}}_k = -\breve{\boldsymbol{\Lambda}}_s^{-1}\breve{\boldsymbol{U}}_s^H\boldsymbol{R}\tilde{\boldsymbol{w}}_k \end{aligned} \tag{59}$$

where $\breve{\boldsymbol{U}}_s^H\overline{\boldsymbol{h}}_k = \mathbf{0}$, and the fourth equality follows from (45). Hence, $\overline{\boldsymbol{w}}_k = \breve{\boldsymbol{U}}_s\boldsymbol{c}_k + \tilde{\boldsymbol{w}}_k = (\boldsymbol{I}_{Pm} - \breve{\boldsymbol{U}}_s\breve{\boldsymbol{\Lambda}}_s^{-1}\breve{\boldsymbol{U}}_s^H\boldsymbol{R})\tilde{\boldsymbol{w}}_k = (\boldsymbol{I}_{Pm} - \breve{\boldsymbol{U}}_s\breve{\boldsymbol{\Lambda}}_s^{-1}\breve{\boldsymbol{U}}_s^H\boldsymbol{R})\tilde{\boldsymbol{H}}(\tilde{\boldsymbol{H}}^H\tilde{\boldsymbol{H}})^{-1}\mathbf{1}_{\tilde{K}\iota+k}$.

Proof of Proposition 3: We first solve for $\tilde{\boldsymbol{m}}_k$ in (46). Since $\tilde{\boldsymbol{m}}_k \in \tilde{\boldsymbol{H}}$, and $\tilde{\boldsymbol{H}}$ has full column rank $\tilde{r}$, we can write $\tilde{\boldsymbol{m}}_k = \tilde{\boldsymbol{H}}\tilde{\boldsymbol{c}}_k$, for some $\tilde{\boldsymbol{c}}_k \in \mathcal{C}^{\tilde{r}}$. Substituting this into (46), we have

$$\begin{aligned}\tilde{\boldsymbol{c}}_k &= \arg\min_{\boldsymbol{c}\in\mathcal{C}^{\tilde{r}}} E\{|b_k[i] - \boldsymbol{c}^H\tilde{\boldsymbol{H}}^H\tilde{\boldsymbol{r}}[i]|^2\}\\ &= \arg\min_{\boldsymbol{c}\in\mathcal{C}^{\tilde{r}}} \boldsymbol{c}^H[\tilde{\boldsymbol{H}}^H(\tilde{\boldsymbol{H}}\tilde{\boldsymbol{H}}^H + \sigma^2\boldsymbol{I}_{Pm})\tilde{\boldsymbol{H}}]\boldsymbol{c}\\ &\quad - 2\Re\{\mathbf{1}^T_{\tilde{K}\iota+k}\tilde{\boldsymbol{H}}^H\boldsymbol{H}\boldsymbol{c}\}\\ &= [(\tilde{\boldsymbol{H}}^H\tilde{\boldsymbol{H}})(\tilde{\boldsymbol{H}}^H\tilde{\boldsymbol{H}}) + \sigma^2\tilde{\boldsymbol{H}}^H\tilde{\boldsymbol{H}}]^{-1}(\tilde{\boldsymbol{H}}^H\tilde{\boldsymbol{H}})\mathbf{1}_{\tilde{K}\iota+k}\\ &= (\tilde{\boldsymbol{H}}^H\tilde{\boldsymbol{H}} + \sigma^2\boldsymbol{I}_{\tilde{r}})^{-1}\mathbf{1}_{\tilde{K}\iota+k}. \end{aligned} \tag{60}$$

Next, we solve $\breve{\boldsymbol{m}}_k = \breve{\boldsymbol{U}}_s\breve{\boldsymbol{c}}_k$ in (59) for some $\breve{\boldsymbol{c}}_k \in \mathcal{C}^{(r-\tilde{r})}$. Following the same derivation as (59), we obtain $\breve{\boldsymbol{c}}_k = -\breve{\boldsymbol{\Lambda}}_s^{-1}\breve{\boldsymbol{U}}_s^H\boldsymbol{R}\tilde{\boldsymbol{m}}_k$. Therefore, we have

$$\begin{aligned}\overline{\boldsymbol{m}}_k &= \breve{\boldsymbol{U}}_s\breve{\boldsymbol{c}}_k + \tilde{\boldsymbol{m}}_k = (\boldsymbol{I}_{Pm} - \breve{\boldsymbol{U}}_s\breve{\boldsymbol{\Lambda}}_s^{-1}\breve{\boldsymbol{U}}_s^H\boldsymbol{R})\tilde{\boldsymbol{H}}\tilde{\boldsymbol{c}}_k\\ &= (\boldsymbol{I}_{Pm} - \breve{\boldsymbol{U}}_s\breve{\boldsymbol{\Lambda}}_s^{-1}\breve{\boldsymbol{U}}_s^H\boldsymbol{R})\tilde{\boldsymbol{H}}(\tilde{\boldsymbol{H}}^H\tilde{\boldsymbol{H}} + \sigma^2\boldsymbol{I}_{\tilde{r}})^{-1}\mathbf{1}_{\tilde{K}\iota+k}. \end{aligned} \tag{61}$$

Proof of Proposition 4: Using the method of Lagrange multiplier to solve the constrained optimization problem (42), we obtain

$$\begin{aligned}\overline{\boldsymbol{d}}_k &= \arg\min_{\boldsymbol{d}\in\text{range}(\boldsymbol{H})} \boldsymbol{d}^H\boldsymbol{H}\boldsymbol{H}^H\boldsymbol{d}\\ &\quad + \Re\{\underline{\lambda}^H(\tilde{\boldsymbol{H}}^H\boldsymbol{d} - \mathbf{1}_{\tilde{K}\iota+k})\}\\ &= (\boldsymbol{H}\boldsymbol{H}^H)^{\dagger}\tilde{\boldsymbol{H}}\underline{\lambda}. \end{aligned} \tag{62}$$

Substituting (62) into the constraint that $\tilde{\boldsymbol{H}}^H\overline{\boldsymbol{d}}_k = \mathbf{1}_{\tilde{K}\iota+k}$, we obtain $\underline{\lambda} = [\tilde{\boldsymbol{H}}^H(\boldsymbol{H}\boldsymbol{H}^H)^{\dagger}\tilde{\boldsymbol{H}}]^{-1}\mathbf{1}_{\tilde{K}\iota+k}$. Hence

$$\begin{aligned}\overline{\boldsymbol{d}}_k &= (\boldsymbol{H}\boldsymbol{H}^H)^{\dagger}\tilde{\boldsymbol{H}}[\tilde{\boldsymbol{H}}^H(\boldsymbol{H}\boldsymbol{H}^H)^{\dagger}\tilde{\boldsymbol{H}}]^{-1}\mathbf{1}_{\tilde{K}\iota+k}\\ &= \boldsymbol{U}_s(\boldsymbol{\Lambda}_s - \sigma^2\boldsymbol{I}_r)^{-1}\boldsymbol{U}_s^H\tilde{\boldsymbol{H}}\\ &\quad \cdot [\tilde{\boldsymbol{H}}^H\boldsymbol{U}_s(\boldsymbol{\Lambda}_s - \sigma^2\boldsymbol{I}_r)^{-1}\boldsymbol{U}_s^H\tilde{\boldsymbol{H}}]^{-1}\mathbf{1}_{\tilde{K}\iota+k} \end{aligned} \tag{63}$$

where the second equality follows from (22) and the fact that $\boldsymbol{U}_n^H\tilde{\boldsymbol{H}} = \mathbf{0}$.

Proof of Proposition 5: Using the method of Lagrange multiplier to solve the relaxed optimization problem (43) over $\boldsymbol{w} \in \mathcal{C}^{Pm}$, we obtain

$$\begin{aligned}\overline{\boldsymbol{w}}_k &= \arg\min_{\boldsymbol{w}\in\mathcal{C}^{Pm}} E\{|b_k[i] - \boldsymbol{w}^H\boldsymbol{r}[i]|^2\}\\ &\quad + \Re\{\tilde{\underline{\lambda}}^H(\tilde{\boldsymbol{H}}^H\boldsymbol{w} - \mathbf{1}_{\tilde{K}\iota+k})\}\\ &= \arg\min_{\boldsymbol{w}\in\mathcal{C}^{Pm}} \boldsymbol{w}^H\boldsymbol{R}\boldsymbol{w} - \Re\{2\overline{\boldsymbol{h}}_k^H\boldsymbol{w}\}\\ &\quad + \Re\{\tilde{\underline{\lambda}}^H(\tilde{\boldsymbol{H}}^H\boldsymbol{w} - \mathbf{1}_{\tilde{K}\iota+k})\}\\ &= \arg\min_{\boldsymbol{w}\in\mathcal{C}^{Pm}} \boldsymbol{w}^H\boldsymbol{R}\boldsymbol{w} + \Re\{\underline{\lambda}^H(\tilde{\boldsymbol{H}}^H\boldsymbol{w} - \mathbf{1}_{\tilde{K}\iota+k})\}\\ &= \boldsymbol{R}^{-1}\tilde{\boldsymbol{H}}\underline{\lambda} \end{aligned} \tag{64}$$

where $\underline{\lambda} \triangleq \tilde{\underline{\lambda}} - 2\mathbf{1}_{\tilde{K}\iota+k}$. Substituting (64) into the constraint that $\tilde{\boldsymbol{H}}^H\overline{\boldsymbol{w}}_k = \mathbf{1}_{\tilde{K}\iota+k}$, we obtain $\underline{\lambda} = (\tilde{\boldsymbol{H}}^H\boldsymbol{R}^{-1}\tilde{\boldsymbol{H}})^{-1}\mathbf{1}_{\tilde{K}\iota+k}$. Hence

$$\begin{aligned}\overline{\boldsymbol{w}}_k &= \boldsymbol{R}^{-1}\tilde{\boldsymbol{H}}[\tilde{\boldsymbol{H}}^H\boldsymbol{R}^{-1}\tilde{\boldsymbol{H}}]^{-1}\mathbf{1}_{\tilde{K}\iota+k}\\ &= \boldsymbol{U}_s\boldsymbol{\Lambda}_s^{-1}\boldsymbol{U}_s^H\tilde{\boldsymbol{H}}[\tilde{\boldsymbol{H}}^H\boldsymbol{U}_s\boldsymbol{\Lambda}_s^{-1}\boldsymbol{U}_s^H\tilde{\boldsymbol{H}}]^{-1}\mathbf{1}_{\tilde{K}\iota+k} \end{aligned} \tag{65}$$

where the second equality follows from (22) and the fact that $\boldsymbol{U}_n^H\tilde{\boldsymbol{H}} = \mathbf{0}$. It is seen that from (65) that $\overline{\boldsymbol{w}}_k \in \text{range}(\boldsymbol{U}_s) = \text{range}(\boldsymbol{H})$; therefore, it is the solution to the constrained optimization problem (43).

Proof of Proposition 6: Since the columns of $\boldsymbol{Q}_s$ form an orthonormal basis of range($\breve{\boldsymbol{U}}_s$), following the same derivation as (61), we have

$$\begin{aligned}\overline{\boldsymbol{m}}_k &= [\boldsymbol{I}_{Pm} - \boldsymbol{Q}_s(\boldsymbol{Q}_s^H\boldsymbol{R}\boldsymbol{Q}_s)^{-1}\boldsymbol{Q}_s^H\boldsymbol{R}]\\ &\quad \cdot \tilde{\boldsymbol{H}}(\tilde{\boldsymbol{H}}^H\tilde{\boldsymbol{H}} + \sigma^2\boldsymbol{I}_{\tilde{r}})^{-1}\mathbf{1}_{\tilde{K}\iota+k}. \end{aligned} \tag{66}$$

Furthermore, we have

$$\begin{aligned}\boldsymbol{Q}_s^H \boldsymbol{R} \boldsymbol{Q}_s &= \boldsymbol{Q}_s^H (\boldsymbol{U}_s \boldsymbol{\Lambda}_s \boldsymbol{U}_s^H + \sigma^2 \boldsymbol{U}_n \boldsymbol{U}_n^H) \boldsymbol{Q}_s \\ &= \boldsymbol{Q}_s^H (\boldsymbol{U}_s \boldsymbol{\Lambda}_s \boldsymbol{U}_s^H) \boldsymbol{Q}_s \\ &= \boldsymbol{Q}_s^H (\check{\boldsymbol{P}} \boldsymbol{U}_s \boldsymbol{\Lambda}_s \boldsymbol{U}_s^H \check{\boldsymbol{P}}) \boldsymbol{Q}_s \\ &= \boldsymbol{Q}_s^H (\check{\boldsymbol{P}} \boldsymbol{U}_s) \boldsymbol{\Lambda}_s (\check{\boldsymbol{P}} \boldsymbol{U}_s)^H \boldsymbol{Q}_s \\ &= \boldsymbol{Q}_s^H [\boldsymbol{Q}_s \quad \boldsymbol{Q}_o] \begin{bmatrix} \boldsymbol{R}_s & \boldsymbol{R}_o \\ 0 & 0 \end{bmatrix} \boldsymbol{\Pi} \boldsymbol{\Lambda}_s \boldsymbol{\Pi}^T \begin{bmatrix} \boldsymbol{R}_s & \boldsymbol{R}_o \\ 0 & 0 \end{bmatrix}^H \\ &\quad \cdot [\boldsymbol{Q}_s \quad \boldsymbol{Q}_o]^H \boldsymbol{Q}_s \\ &= \boldsymbol{R}_s \boldsymbol{\Pi} \boldsymbol{\Lambda}_s \boldsymbol{\Pi}^T \boldsymbol{R}_s^H \end{aligned} \tag{67}$$

where the second equality follows from $\boldsymbol{U}_n^H \boldsymbol{Q}_s = \boldsymbol{0}$, the third equality follows from $\check{\boldsymbol{P}} + \tilde{\boldsymbol{P}} = \boldsymbol{I}_{Pm}$ and $\tilde{\boldsymbol{P}} \boldsymbol{Q}_s = \boldsymbol{0}$, and the fifth equality follows from (53). Substituting (67) into (66) we obtain (54).

Proof of Proposition 7: Following the same derivation as in (64), we have

$$\begin{aligned}\overline{\boldsymbol{w}}_k^j &= \boldsymbol{R}_{jj}^{-1} \tilde{\boldsymbol{H}} (\tilde{\boldsymbol{H}}^H \boldsymbol{R}_{jj}^{-1} \tilde{\boldsymbol{H}})^{-1} \boldsymbol{1}_{\tilde{K}\iota+k} \\ &= \boldsymbol{L}^j \boldsymbol{L}^{jH} \tilde{\boldsymbol{H}} (\tilde{\boldsymbol{H}}^H \boldsymbol{L}^j \boldsymbol{L}^{jH} \tilde{\boldsymbol{H}})^{-1} \boldsymbol{1}_{\tilde{K}\iota+k} \\ &= \boldsymbol{L}_s^j \boldsymbol{L}_s^{jH} \tilde{\boldsymbol{H}} (\tilde{\boldsymbol{H}}^H \boldsymbol{L}_s^j \boldsymbol{L}_s^{jH} \tilde{\boldsymbol{H}})^{-1} \boldsymbol{1}_{\tilde{K}\iota+k} \end{aligned} \tag{68}$$

where the second equality follows from the definition in (31) and the last equality follows from (32) and the fact that $\boldsymbol{L}_n^{jH} \tilde{\boldsymbol{H}} = \boldsymbol{0}$.

REFERENCES

[1] T. W. Anderson, *An Introduction to Multivariate Statistical Analysis*. New York: Wiley, 1984.

[2] A. N. Barbosa and S. L. Miller, "Adaptive detection of DS/CDMA signals in fading channels," *IEEE Trans. Commun.*, vol. 46, pp. 115–124, Jan. 1998.

[3] S. E. Bensley and B. Aazhang, "Subspace-based channel estimation for code-division multiple-access communication systems," *IEEE Trans. Commun.*, vol. 44, pp. 1009–1020, Aug. 1996.

[4] R. D. DeGroat, E. M. Dowling, and D. A. Linebarger, "Subspace tracking," in *The Digital Signal Processing Handbook*, V. K. Madisetti and D. B. Williams, Eds. Piscataway, NJ: IEEE Press, 1998.

[5] G. H. Golub and C. F. Van Loan, "Matrix computations," 2nd ed., Baltimore, MD: Johns Hopkins Univ. Press, 1989.

[6] M. Honig, U. Madhow, and S. Verdú, "Blind adaptive multiuser detection," *IEEE Trans. Inform. Theory*, vol. 41, pp. 944–960, July 1995.

[7] M. Honig and H. V. Poor, "Adaptive interference suppression," in H. V. Poor and G. W. Wornell, Eds., *Wireless Communications: A Signal Processing Perspective*. Upper Saddle River, NJ: Prentice Hall, 1998, pp. 64–128.

[8] A. Høst-Madsen, "Semi-blind multiuser detectors for CDMA: Subspace methods," Tech. Rep., TR Labs, University of Calgary, Calgary, Canada.

[9] A. Høst-Madsen and K.-S. Cho, "MMSE/PIC multi-user detection for DS/CDMA systems with inter- and intra-interference," *IEEE Trans. Commun.*, vol. 47, pp. 291–299, Feb. 1999.

[10] A. Høst-Madsen and J. Yu, "Hybrid semi-blind multiuser detection: Subspace tracking method," in *Proc. 1999 IEEE ICASSP*, pp. III.352–III.355.

[11] H. C. Huang and S. Verdu, "Linear differentially coherent multiuser detection for multipath channels," *Wireless Personal Commun.*, vol. 6, pp. 113–136, Jan. 1998.

[12] H. Liu and G. Xu, "A subspace method for signal waveform estimation in synchronous CDMA systems," *IEEE Trans. Commun.*, vol. 44, pp. 1346–1354, Oct. 1996.

[13] U. Madhow, "Blind adaptive interference suppression for the near-far resistant acquisition and demodulation of direct-sequence CDMA signals," *IEEE Trans. Signal Proc.*, vol. 45, Jan. 1997, pp. 124–136.

[14] ——, "Blind adaptive interference suppression for CDMA," *Proc. IEEE*, vol. 86, Oct. 1998, pp. 2049–2069.

[15] H. V. Poor and X. Wang, "Code-aided interference suppression in DS/CDMA communications—Part II: Parallel blind adaptive implementations," *IEEE Trans. Commun.*, vol. 45, pp. 1112–1122, Sept. 1997.

[16] ——, "Blind adaptive suppression of narrowband digital interferers from spread-spectrum signals," *Wireless Personal Commun.*, vol. 6, pp. 69–96, Jan. 1998.

[17] Y. Song and S. Roy, "Blind adaptive reduced-rank detection for DS-CDMA signals in multipath channels," *IEEE Trans. Commun.*, to be published.

[18] M. Torlak and G. Xu, "Blind multiuser channel estimation in asynchronous CDMA systems," *IEEE Trans. Signal Processing*, vol. 45, pp. 137–147, Jan. 1997.

[19] M. K. Tsatsanis, "Inverse filtering criteria for CDMA systems," *IEEE Trans. Signal Processing*, vol. 45, pp. 102–112, Jan. 1997.

[20] M. K. Tsatsanis and G. B. Giannakis, "Blind estimation of direct sequence spread spectrum signals in multipath," *IEEE Trans. Signal Processing*, vol. 45, pp. 1241–1252, May 1997.

[21] S. Verdú, *Multiuser Detection*. Cambridge, UK: Cambridge Univ. Press, 1998.

[22] X. Wang and H. V. Poor, "Adaptive joint multiuser detection and channel estimation in multipath fading CDMA channels," *ACM/Baltzer Wireless Networks*, pp. 453–470, 1998.

[23] ——, "Blind adaptive multiuser detection in multipath CDMA channels based on subspace tracking," *IEEE Trans. Signal Processing*, vol. 46, pp. 3030–3044, Nov. 1998.

[24] ——, "Blind equalization and multiuser detection for CDMA communications in dispersive channels," *IEEE Trans. Commun.*, vol. 46, pp. 91–103, Jan. 1998.

[25] ——, "Blind multiuser detection: A subspace approach," *IEEE Trans. Inform. Theory*, vol. 44, pp. 677–691, Mar. 1998.

[26] ——, "Blind joint equalization and multiuser detection for DS-CDMA in unknown correlated noise," *IEEE Trans. Circuits Syst. II*, vol. 46, pp. 886–895, July 1999.

[27] ——, "Robust multiuser detection in non-Gaussian channels," *IEEE Trans. Signal Processing*, vol. 47, pp. 289–305, Feb. 1999.

[28] Q. Wu and K. M. Wong, "UN-MUSIC and UN-CLE: An application of generalized correlation analysis to the estimation of the direction of arrival of signals in unknown correlated noise," *IEEE Trans. Signaling Processing*, vol. 42, pp. 2331–2343, Sept. 1994.

[29] L. J. Zhu and U. Madhow, "Adaptive interference suppression for direct sequence CDMA over severely time-varying channels," in *Proc. IEEE Globecom'97*, pp. 917–922.

Xiaodong Wang (S'98–M'98) received the M.S. degree in electrical and computer engineering from Purdue University, West Lafayette, IN, in 1995, and the Ph.D. degree in electrical engineering from Princeton University, Princeton, NJ, in 1998.

In July 1998, he joined the Department of Electrical Engineering, Texas A&M University, as an Assistant Professor.

His research interests fall in the general aeras of computing, signal processing, and communications. His current research interests include multiuser communications theory and advanced signal processing for wireless communications.

Dr. Wang has received the 1999 National Science Foundation CAREER Award.

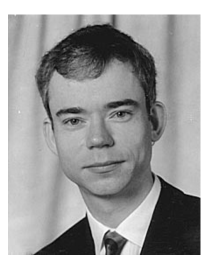

Anders Høst-Madsen (M'95) was born in Denmark in 1966. He received the M.Sc. degree in electrical engineering in 1990 and the Ph.D. degree in mathematics in 1993, both from the Technical University of Denmark.

From 1993 to 1996, he was with Dantec Measurement Technology A/S, Denmark, and from 1996 to 1998, he was an Assistant Professor at Kwangju Institute of Science and Technology, Korea. He is currently an Assistant Professor in the Department of Electrical and Computer Engineering, University of Calgary, Canada, and a Staff Scientist at TR Labs, Calgary, Canada. He has also been a Visitor at the Department of Mathematics, University of California, Berkeley, through 1992. His research interests are in statistical signal processing and applications to wireless communications, including multiuser detection, equalization, and echo cancellation.